

NORMAL AND SHEAR FORCE MEASUREMENT AND ANALYSIS
FOR THE THREE AXIS CAPACITIVE TACTILE SENSOR

by

Kyungjin Park

A thesis submitted to the faculty of
The University of Utah
in partial fulfillment of the requirements for the degree of

Master of Science

Department of Electrical and Computer Engineering

The University of Utah

December 2013

Copyright © Kyungjin Park 2013

All Rights Reserved

THE UNIVERSITY OF UTAH GRADUATE SCHOOL

STATEMENT OF THESIS APPROVAL

The thesis of Kyungjin Park
has been approved by the following supervisory committee members:

Carlos Mastrangelo , Chair 09/26/2013
Date Approved

Darrin Young , Member 09/26/2013
Date Approved

Gianluca Lazzi , Member 09/26/2013
Date Approved

and by Gianluca Lazzi , Chair of
the Department of Electrical and Computer Engineering

and by David B. Kieda, Dean of The Graduate School.

ABSTRACT

To get reliable location and time information for specific objects, the U. S. Department of Defense (DOD) developed the Global Positioning System (GPS). In spite of its enormous advantages, it encounters limitations in GPS-denied or compromised environments. To address these limitations, Inertial Motion Units (IMUs), consisting of gyroscopic devices, have been substituted for GPS in these harsh environments. However, they are also limited by bias, which increases error growth by integrating signals. This research project allows for tracking a pedestrian in GPS-limited environments by adding another portable localization system to the IMU, the Ground Reaction Sensor Cluster (GRSC). The GRSC measures the precise velocity of an object by applying zero velocity updating (ZUPTing) events, and seeks to compensate for the limitations of the IMU to give the precise position of the pedestrian. This project addresses the testing environment developed to evaluate the reliability of a shoe-mounted GRSC. This environment consisted of both physical measurements and analysis of the data. Through this testing, we check whether this device would meet the Defense Advanced Research Projects Agency's (DARPA) requirement to resolve the zero-velocity error biases of 4000, 250 and 20 $\mu\text{m/s}$ with a typical 0.3s midstance measurement time. To ensure an adequate amount of data, the process was automated and run for several different cycle lengths.

To my beloved parents and sister Minkyong,
and my old friend Keith

TABLE OF CONTENTS

ABSTRACT.....	iii
LIST OF FIGURES	vii
ACKNOWLEDGMENTS	ix
CHAPTERS	
1. OVERVIEW OF PROJECT	1
Introduction.....	1
Need of Ground Reaction Sensor Cluster (GRSC).....	3
Testing Environment.....	5
2. BACKGROUND OF THE SENSOR	7
Materials of GRSC.....	7
Structure of the Sensor.....	7
Capacitance Nonlinearity Analysis.....	9
Advantages of Ground Reaction Sensor Cluster (GRSC)	13
3. INTRODUCTION OF TESTING.....	15
The Role and Benefits of Testing	15
General Testing Steps	15
4. NORMAL AND SHEAR FORCE TESTING EQUIPMENT.....	18
Hardware.....	18
Motion of Each Stage	21
Coarse Testing	25
5. STRESS TESTING.....	26
Introduction.....	26
Data Control.....	27
Testing Equipment.....	30
Data Analysis	31
6. INTEGRATION AND AUTOMATION.....	35

Introduction.....	35
Physical Setup Movement Control	36
Data Control.....	37
7. DATA ANALYSIS AND CONCLUSION	44
Data Analysis	44
Conclusion	48
APPENDIX: SAMPLE CODE OF VISUAL BASIC .NET FOR STRESS TESTING...	49
REFERENCES	53

LIST OF FIGURES

1.1. Stance phase in human bipedal locomotion.....	4
2.1. Top view of Ground Reaction Sensor Cluster (GRSC)	8
2.2. Cross section of single unit	8
2.3. Real and estimated shape	10
2.4. Assumed shape of single unit	10
2.5. Movement of single electrode detector.....	10
2.6. Cross section of assumed detector	11
2.7. Moved single detector by force.....	11
3.1. Testing process.....	16
4.1. Implementation diagram of 3 axis linear stage	19
4.2. Normal force sensor gage	22
4.3. Shear force measurement graph.....	22
4.4. Automated 3 axis linear stage for GRSC testing	24
5.1. Data flow diagram.....	29
5.2. Stress testing setup	32
5.3. Realization of stress testing setup	32
5.4. Reliability of wire under a very large number of bending cycles	33
5.5. Ten pair of sample cycle	34
6.1. Normal and shear force measurement.....	37

6.2. Data control structure diagram.....	38
6.3. AD 7746 evaluation and MINT-CV-M1 extension board.....	40
6.4. User interface control terminal	43
6.5 Sample code for DDE	43
7.1. Reference measurement without PDMS	45
7.2. Reference measurement without PDMS	45
7.3. Mapping with 0.8 lb weight	46
7.4. Mapping with three weights.....	47
7.5. Mapping with six weights.....	47

ACKNOWLEDGMENTS

This thesis would not have been possible without the support of my advisor, Carlos Mastrangelo, who provided me with a valuable opportunity to conduct research in MEMs. He guided me through this project and gave tremendous advice that allowed me to follow a productive path and achieve reliable results. Thank you for your patience. Likewise, I am grateful to my committee members, Darrin Young and Gianluca Lazzi, who offered guidance and correction. Also, thanks to my colleague, Rajesh Surapaneni, who provided his expertise by fabricating the sensor. It was a pleasure to collaborate with you on this project. I also want to remember my college Yan Xie, who gave me valuable tips on how to deal with equipment in the FAB. I would like to acknowledge DARPA (Defense Advanced Research Projects Agency), which provided funding for our ongoing research.

I am indebted to mentors and friends, Rowland, Byeongkyun, Qday, Inhee, Jake, Inho, Junbum, Tearim, Jongwon, Hyunwook, Hyunjun, Giyun, Ben, and many others. I especially want to show my appreciation to my old Kimchi, Keith Phenny, who helped, supported, and encouraged me to finish this thesis, demonstrating his long-lasting friendship.

Finally, I owe the greatest thanks to my parents and my sister, who have shown me unchanging love, strong support, and intimate fellowship. Above all, I give all my thanks to God.

CHAPTER 1

OVERVIEW OF PROJECT

Introduction

Disasters such as wars, terrorist attacks, tsunamis, or earthquakes seem to be getting more frequent. To address these situations, soldiers and first responders must work in unsafe and sometimes life-threatening environments.

It is a significant issue to track soldiers working in subterranean environments in Afghanistan, where the Global Positioning Satellite (GPS) signal cannot reach the theater of the mission. Tracking first responders is also another important issue as they are sent to the places where buildings have been destroyed from terrorist attacks. Following natural disasters, those responders must often work under water, underground or even under thick concrete where bridges or sea ports have collapsed because of a tsunami or an earthquake. The scope of the operation sometimes extends beyond the limit where a GPS signal can reach because of intended jamming.

The GPS navigation system has taken an important role to find a position and to realize real-time tracking systems for humans or vehicles for the military and commercial use. However, GPS signals are highly vulnerable to intended jamming or natural interference. Successful communication with the person or object is not guaranteed in a harsh environment.

From the early 21st century, the Defense Advanced Research Projects Agency (DARPA) has been looking for researchers and institutes who could manufacture autonomous navigation platforms with micro-gyroscopes installed without using GPS signal. It should be small enough to be wearable for soldiers and implanted to specialized utilities such as unmanned vehicles.

Inertial navigation systems (INS) have emerged to compensate for the limitations of the GPS platform. One of the main benefits of INS over GPS is autonomy. It is not dependent on any external resources or on visual assistance; hence, it can work in GPS-denied environments such as tunnels or underwater. Inertial motion units (IMU) is an essential component of an INS that measures acceleration and rotational velocity of the objects while its IMU measures the derivatives of the variables such as position, velocity, and attitude. This underlying characteristic is also good for navigation of the targeted object. Also, since INS does not require an external antenna, and it neither receives nor emits detectable radiation, it is therefore less detectable and more resistant to jamming from others.

In real situations, there are several significant drawbacks to applying portable equipment. Mean-square errors grow according to the operating time, which is critical to perform in an independent platform for a long time. Cost is another issue for individual use. Electromechanical systems have higher failure rates and maintenance cost than electronic systems like GPS. Time to initialize position and attitude of INS by gyrocompass alignment also takes several minutes. Even though the MEMS technology has been able to shrink size, weight, power consumption, and heat dissipation of the

system and device, micro and nano-scale systems and devices still have some area to work on size, weight, and power consumption.

Some of the most critical issues are the bias and drift rates in the gyros with increasing tilt error. The vertical acceleration error is 9.8 m/s^2 times the tilt error. This double integrating position error is proportional to the quadrature or the cube in a few seconds [1-4]. Kinematic motion information for a short term could be useful to hold this timely increasing error. A human's walking motion has a stationary phase before and after the swing stride phase. With this information, timely increasing error is bounded. This is called zero-velocity updates (ZUPTs).

Detecting the stationary phase is key to zero-velocity updates to minimize the error growth of a shoe-based INS. Motion of each gate cycle is important, as the variables such as the velocity, position, speed and the yaw will be reset to zero. The roll and pitch of the object also will be initialized from Inertial Measurement Units (IMUs) to limit the growth error [5, 6].

To detect the stationary phase of foot motion to apply zero-velocity updates, using biomechanical ground reaction sensor clusters (GRSC) is best addressed, as shown in Figure 1.1, for zero-velocity updating inertial measurement navigation units (IMUs).

Need of Ground Reaction Sensor Cluster (GRSC)

Recent inertial navigation systems have been constructed with dead reckoning, magnetometry, and GPS data to reduce timely increasing IMU errors. Dead reckoning finds out current and future locations from past and current locations using previous information of steering courses and speed. A step-based position measurement technique has been sought for use by pedestrians, using dead reckoning. To calculate its steps, they

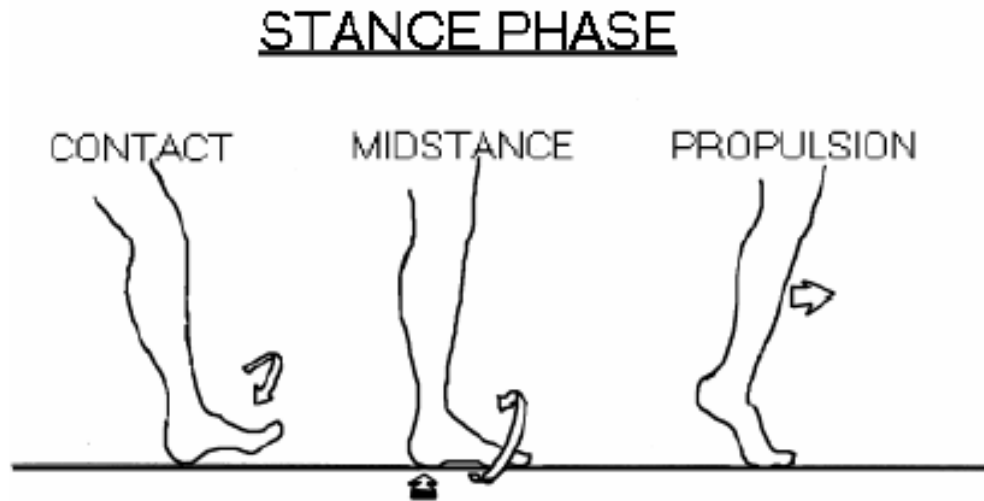


Figure 1.1: Stance phase in human bipedal locomotion

have made use of pedometers and accelerometers [7]. The problem here is if there is no fix for a certain amount of time, the error will be accumulated proportional to time. This time-dependent error is significant so that the navigator should reset and update the estimated position when the velocity of the object is zero [8]. INS using dead reckoning (also known as step-correction) has been successful catching the zero-velocity phases. However, the resolution of it is not so high that it only detects the step impact shock with accelerometers that are located away from the ground. This module only recognizes the beginning of the stance phase by detecting shock when the foot starts to touch the ground. The main role of GRSC is measuring dynamic ground forces of the sole contact (or plantar) pressure, shear strains, and sole mechanical deformation. GRSC provides rich information that makes it possible to design a biomechanical foot motion model. High-resolution data provides accurate periods of zero velocity. In turn, these accurate zero

velocity points make discrete velocity corrections (ZUPTing), and correcting IMU error brings in increasingly effective positioning resolution.

GRSC data themselves cannot tell us the position of the zero velocity, but by combining the recursive detection data of pressure and shear force which come from the capacitive tactile sensor, we can match the GRSC data to well-defined biomechanical model data. An accurate biomechanical model specifies the relationship between the velocity at the IMU location and the GRSC data. GRSC data are sent to an external computer to calculate the ground contact velocity and rotation resolution. A biomechanical mathematical model transfers the planar pressure and stress data to reading of the zero velocity in IMU. In this manner, GRSC can be combined with IMU-based navigation systems.

Testing Environment

Through testing, reliability of the device could be evaluated in real situations. Problems in real environments could be predicted by comparing theoretical and experimental results. By predicting the problems posed in the current device, defective devices could be modified in earlier stages of fabrication to eliminate or minimize expected problems in real situations. This brings about time savings in the whole project schedule, and is beneficial to budget.

Since this project was sponsored by DARPA, proving the reliability in real environments was critical to retain the on-going project. Through this testing, we check whether this device would work the way we designed it to meet DARPA's requirement to resolve the zero-velocity error biases of 4000, 250, and 20 $\mu\text{m/s}$ with a typical 0.3s midstance measurement time.

As one of the milestones, rich information is necessary to make an accurate biomechanical model for a motion of the gait. If some part of the device is not properly working, then it loses a set of data connected onto it. Loss of some information limits getting the rich information of a gait motion. This is why testing, finding an error, and modifying the fabrication process are critical.

CHAPTER 2

BACKGROUND OF THE SENSOR

Materials of GRSC

Among a range of materials, a soft surface is desirable for tactile sensors in terms of its impact energy attenuation, surface conformability, and strain energy dissipation [9, 10]. In this project, Polydimethylsiloxane (PDMS) is used as the dielectric material which is the most commonly used silicon-based organic polymer in MEMS. PDMS dielectric constant ranges between 2.3-2.8. According to Knovel Critical Tables, the minor disadvantage of PDMS for military purposes is the low melting point around 40° [11, 12]. Gold is used as electrodes, on the top and bottom side of the dielectric material.

Structure of the Sensor

As shown in Figure 2.1, a tactile capacitive sensor has been used as a ground reaction sensor cluster to measure the pressure and shear distribution. Each unit has two detectors placed perpendicular to each other according to the x, y direction. This sensor is based on a flexible dielectric material (PDMS) with conductive material (gold) – an octagon shaped layer at the bottom and two half-octagon shaped layers at the top, as shown in Figure 2.2.

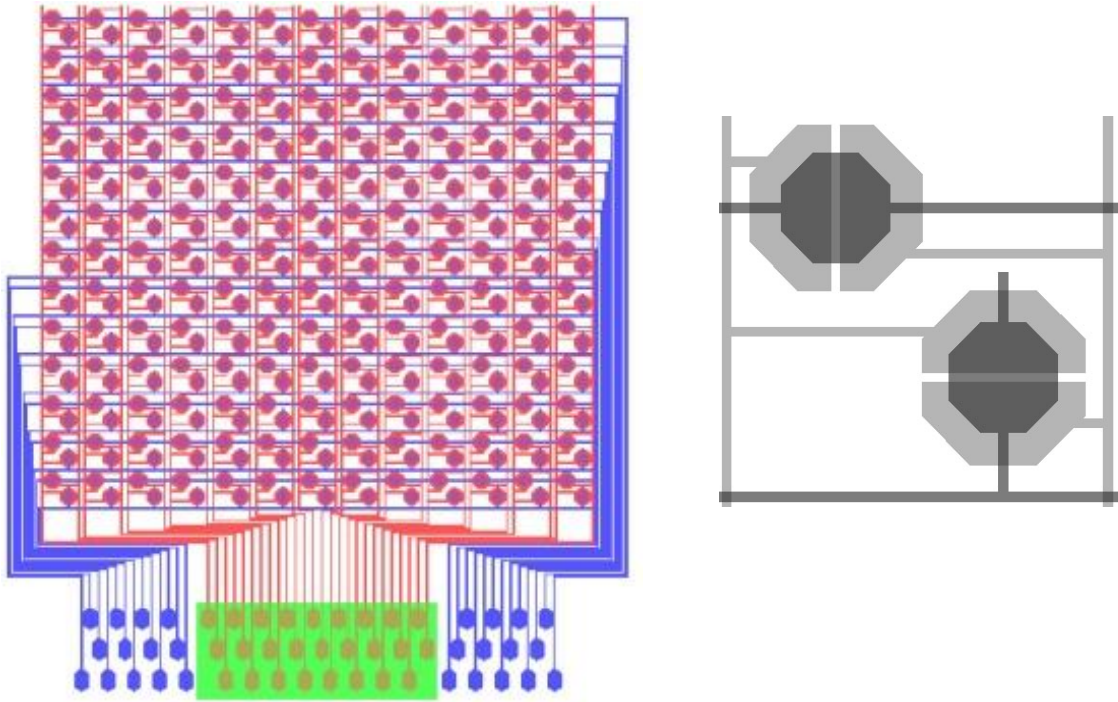


Figure 2.1: Top view of Ground Reaction Sensor Cluster (GRSC)¹

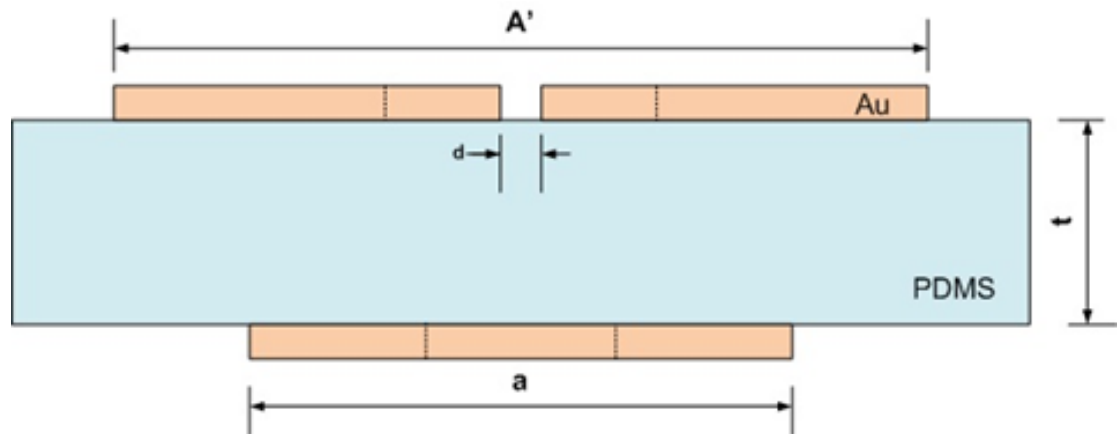


Figure 2.2: Cross section of single unit

¹ GRSC sensor was fabricated by my colleague, Rajesh Surapaneni

Capacitance Nonlinearity Analysis

In the design and calculation step, it is assumed that the shape of the electrodes on top and bottom of the dielectric material are round. However, the actual shape of the electrodes on both sides is designed to be octagon shaped instead of a circle due to the fabrication limitation, as shown in Figure 2.3. According to calculations, the diameter of the circle ($2R$) is longer than the cross length (A) of the octagon which is considered in the fabrication process.

$$2R > A \dots\dots (1)$$

At the original position without external forces, four sections of the electrodes in the unit detector have the same capacitance. In Figure 2.4, C_1 is the capacitance of the overlapped area on the left side, and C_2 is the capacitance of the overlapped area on the right side. In the same manner, C_3 is the capacitance of the overlapped area on the top side, and C_4 is the capacitance of the overlapped area on the bottom side.

$$C_1 = C_2 = C_3 = C_4 = \frac{\epsilon_0 \epsilon_r A}{t} \dots\dots (2)$$

In case of Figure 2.5 which has an applied force on the $+x$ direction, the area of C_1 is increased while C_2 is decreased. In this case, the area of C_3 and C_4 is not changed, so $S1$ and $S2$ are calculated below. In Figure 2.6 and 2.7, h is the height of the dielectric material, and d is the gap between the two electrodes on the top.

In case of Figure 2.5 (c) which has an applied force on the $+y$ direction, the area

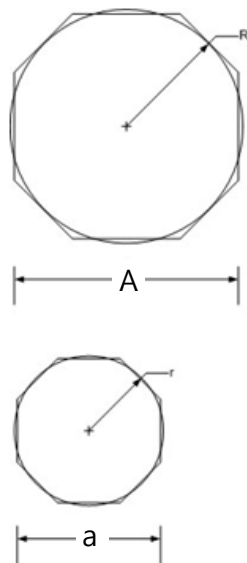


Figure 2.3: Real and estimated shape

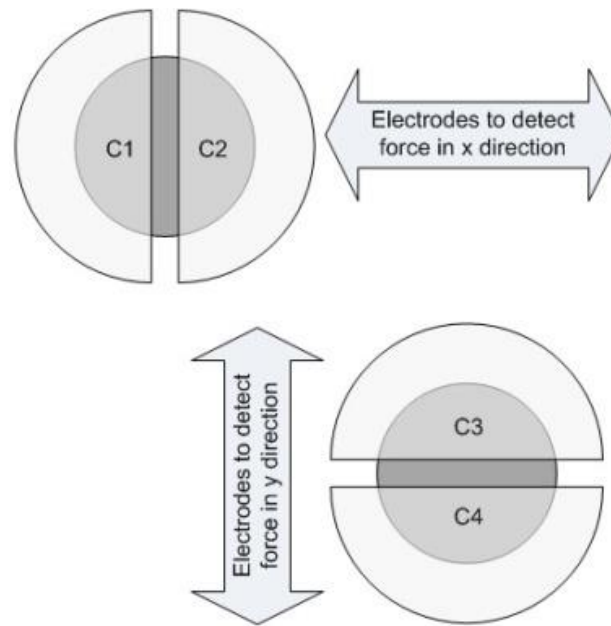


Figure 2.4: Assumed shape of single unit

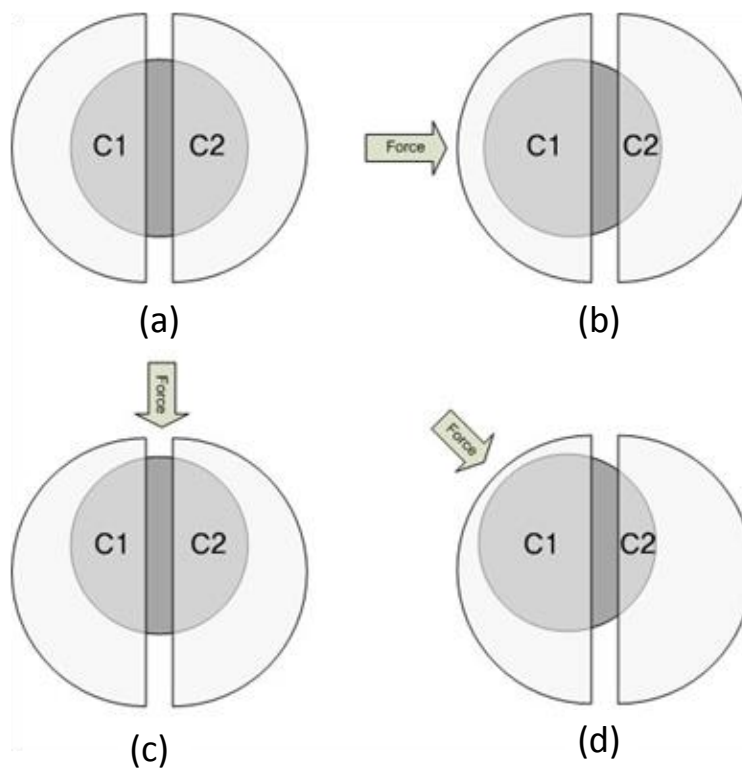


Figure 2.5: Movement of single electrode detector

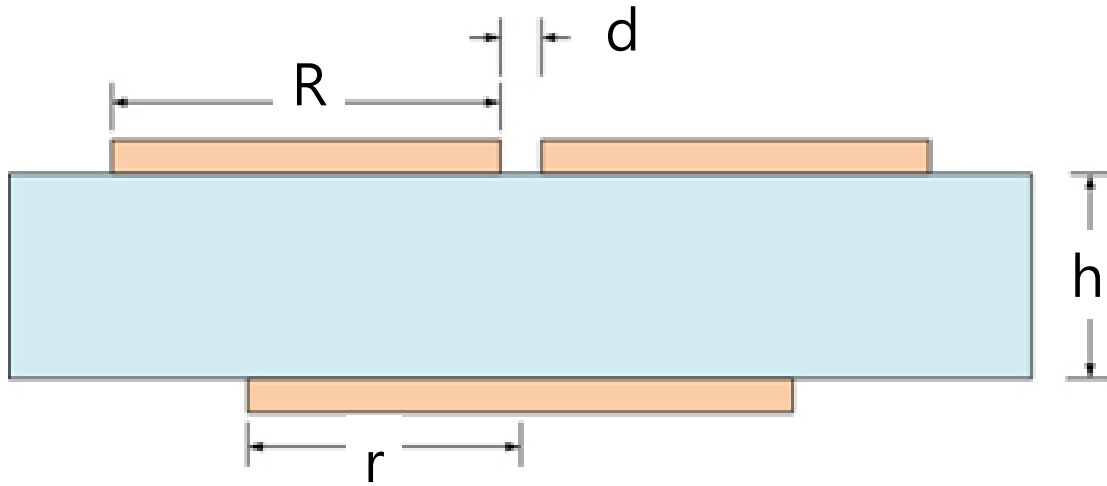


Figure 2.6: Cross section of assumed detector

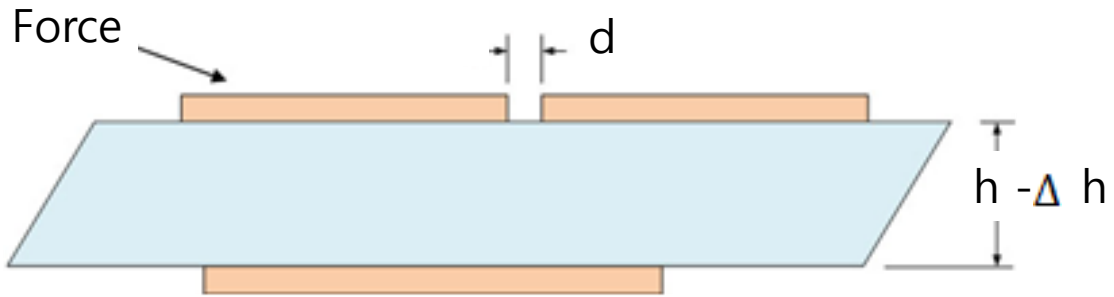


Figure 2.7: Moved single detector by force

$$\begin{aligned}
 S1 &= 2 \times \int_{-r}^{\Delta x - \frac{d}{2}} \sqrt{r^2 - x^2} dx \\
 &= \frac{\pi r^2}{2} + \left(\Delta x - \frac{d}{2} \right) \sqrt{r^2 - (\Delta x - d/2)^2} + r^2 \cdot \sin^{-1} \left(\frac{\Delta x - d/2}{r} \right) \dots\dots (3)
 \end{aligned}$$

$$\begin{aligned}
 S2 &= 2 \times \int_{\Delta x + d/2}^r \sqrt{r^2 - x^2} dx \\
 &= \frac{\pi r^2}{2} - \left(\Delta x + \frac{d}{2} \right) \cdot \sqrt{r^2 - (\Delta x + d/2)^2} + r^2 \cdot \sin^{-1} \left(\frac{\Delta x + d/2}{r} \right) \dots\dots (4)
 \end{aligned}$$

of C_3 is increased while C_4 is decreased. In this case, the area of C_1 and C_2 is not changed, so only $S3$ and $S4$ are calculated. In the same manner of the previous calculation from equation (3) and (4), we could get the area of $S3$ and $S4$.

$$S3 = \frac{\pi r^2}{2} + \left(\Delta y - \frac{d}{2}\right) \sqrt{r^2 - (\Delta y - d/2)^2} + r^2 \cdot \sin^{-1} \left(\frac{\Delta y - d/2}{r} \right) \dots\dots (5)$$

$$S4 = \frac{\pi r^2}{2} - \left(\Delta x + \frac{d}{2}\right) \cdot \sqrt{r^2 - (\Delta x + d/2)^2} + r^2 \cdot \sin^{-1} \left(\frac{\Delta x + d/2}{r} \right) \dots\dots (6)$$

All the above four equations can be used for the case of Figure 2.5 (d) when the force is applied in x and y direction at the same time, which is the almost every case.

As depicted in the previous section, there are two sets of electrodes according to the directions. In Figure 2.5, the movement of a single electrode detector is described by the external forces. Here, the vertical displacement caused by the pressure is described.

$$h = \sqrt{\Delta x^2 + \Delta y^2} \dots\dots (7)$$

$$\Delta h = h(1 - \cos \theta) \dots\dots (8)$$

$$\theta = \sin^{-1} \left(\frac{h}{d} \right) = \sin^{-1} \left(\frac{\sqrt{\Delta x^2 + \Delta y^2}}{d} \right) \dots\dots (9)$$

Angle θ is derived from the horizontal displacement and initial height of the dielectric material. These three equations (Eq. 7-9) can be used to relate capacitance between two electrodes with vertical displacement caused by applied pressure [13].

Advantages of Ground Reaction Sensor Cluster (GRSC)

The main component of the GRSC is a flexible substrate consisting of an array of pressure and shear force sensors. DARPA's requirement is to get the resolution of zero-velocity error biases of 4000, 250, and 20 $\mu\text{m/s}$ with a typical 0.3s midstance measurement time. There are three technical benefits in terms of structure and manufacture aspects in terms of high density, location, and analog sensors.

High Density

A GRSC array with high density could measure the velocity precisely as low as 10 $\mu\text{m/s}$. This high-density GRSC array provides rich data, which makes it possible to get high positioning resolution.

Location

IMU positioning errors are proportional to the square of the measurement interval. Recent inertial navigation systems using dead reckoning (also known as step-correction) detects the step impact shock with accelerometers which are located away from the ground. GRSC sensors are placed at the sole of soldiers' boots close to the ground. It is more sensitive to the ground conditions as it is located at the contact points directly; hence, they could measure precise ground velocity. Close location between GRSC and IMU indicates the close mechanical relation between the velocity at the GRSC and IMU locations. This mechanical proximity reduces the error originated from IMUs and compensates for it.

Analog Sensors

The resolution required in ZUPTing is directly related with the GRSC sensor pitch requirements. Analog sensors increase the pitch gap between the sensors compared to digital determination. In digital sensors, when a pressure is applied, each sensor would give on and off signals at the point of rolling contact between adjacent sensors alike Boolean representation (0 and 1) that represent two states of voltage level.

Analog readouts allow sensors to have lower density which means lower resolution of contact points by interpolating the data of adjacent sensors. For example, velocity change of $20 \mu\text{m/s}$ at sampling rate of 20 ms requires $1 \mu\text{m}$ pitch. Zero-velocity error bias is equal to pitch divided by period (pitch/T_s) which is midstance measurement time in this case. In an analog scale of 8bits or 256 divisions, the sensor pitch requirement is $256 \mu\text{m}$.

To meet project requirements, minimum linear sensor pitch of 1200, 75, and $6 \mu\text{m}$ is required according to zero-velocity error biases of 4000, 250, and $20 \mu\text{m/s}$. If an average heel area is 60 cm^2 , the numbers of sensors in this full coverage area are 49,800, 237,000, and 2.96 million according to these zero-velocity error biases of 4000, 250, and $20 \mu\text{m/s}$.

The analog readout is realized by capacitive sensing that provides linearity to the system. It also achieves low power consumption and is relatively temperature independent. Determination of slippage and shoe rotation estimation is achieved by measuring shear force. The structure of the sensor takes a role for measuring shear force.

CHAPTER 3

INTRODUCTION OF TESTING

The Role and Benefits of Testing

To build up the suitability for a given application, evaluation of a device is essential. To test the sensor, it is fundamental to consider the real environments where the sensor will be used. Carefully designed testing enables researchers to determine how much endurance and resistance the sensor must have in real environments.

A rigorous testing process also makes it possible to anticipate the various error terms for particular circumstances. Recognition of the problems posed by the device gives the direction of how to modify the design of the sensors.

Mathematical expression, as described in Chapter 2, interprets the behavior of the sensor according to the various amount of pressure applied in different directions. By means of applying the mathematical expression to data from the testing result, the relation was clarified between capacitance and vertical displacement caused by pressure.

General Testing Steps

In this project, three typical testing steps are followed - coarse testing, accuracy testing, and final testing. Figure 3.1 describes these three testing steps.

In coarse testing, the device is initially tested with simple methods to obtain broad results. This enables researchers to determine whether the mechanism of the device is

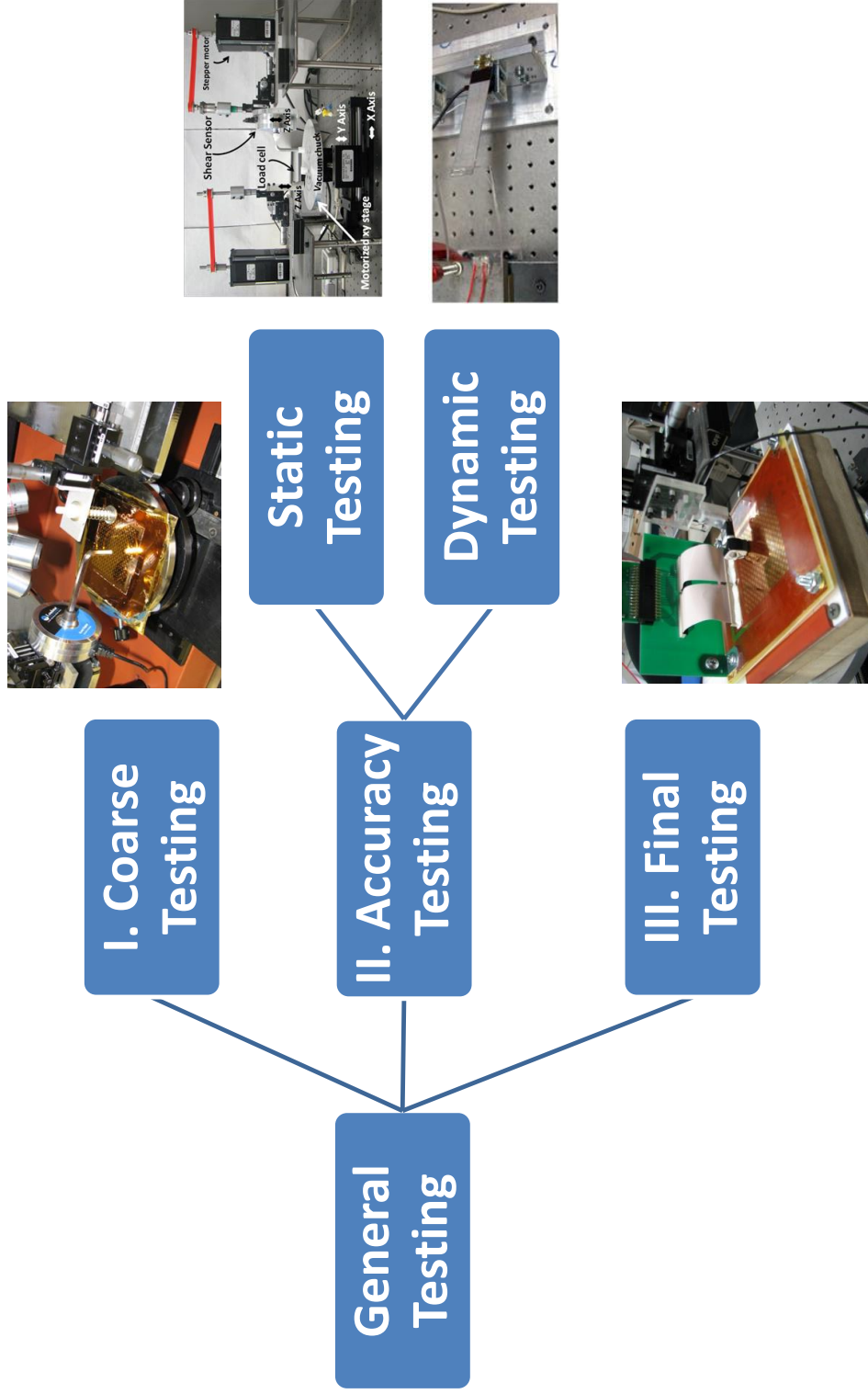


Figure 3.1: Testing process

well-matched with the expectations of it.

Next is accuracy testing. In this step, the device is put on the more accurate and well-organized test bench to make certain that this device meets the requirements. Two different testing steps are normally presented in this process; static testing and a dynamic testing. Static testing specifies the characteristic and performance figure. In this step, the device is fixed to see the response to a certain force or factors. In dynamic testing, on the other hand, the endurance and resistance of the device is checked by applying recursive external forces or factors, and forcing the device to move.

Last is final testing. A sensor is connected with many peripheral devices collaborated with many other groups. This step makes the device fit the user-convenient module by modifying the device to be compatible with the user's requirements.

CHAPTER 4

NORMAL AND SHEAR FORCE TESTING EQUIPMENT

The testing environment is categorized into two parts; hardware and software. Hardware is comprised of three main parts; linear stage, measuring equipment, and controller. Linear stages include the XY linear stage and two Z axis platforms, as shown in Figure 4.1. All of x, y, and z axis movements are important, since precise directional control is required. Measurement equipment is composed of two load sensors and an LCR meter.

Hardware

XY Linear Stage

The main stage requires quick and precise positioning of light payloads. Two linear platforms are crossed in a perpendicular direction. There is a chuck on top of the X-Y linear stage for the sample to be put on. Each linear platform for the XY stage is motorized by the NEMA 17 stepper motor. The resolution of the linear platform is 0.04 μm , and the pitch of the lead screw is 2 mm with 250 μm steps. The maximum speed is 40 mm/sec which is fast enough to run numerous cycles in a short period.

Z Axes Platform

A Z axis linear platform is laid on both the right and the left side of the main XY linear stage. Two individual platforms are employed for both shear and normal force.

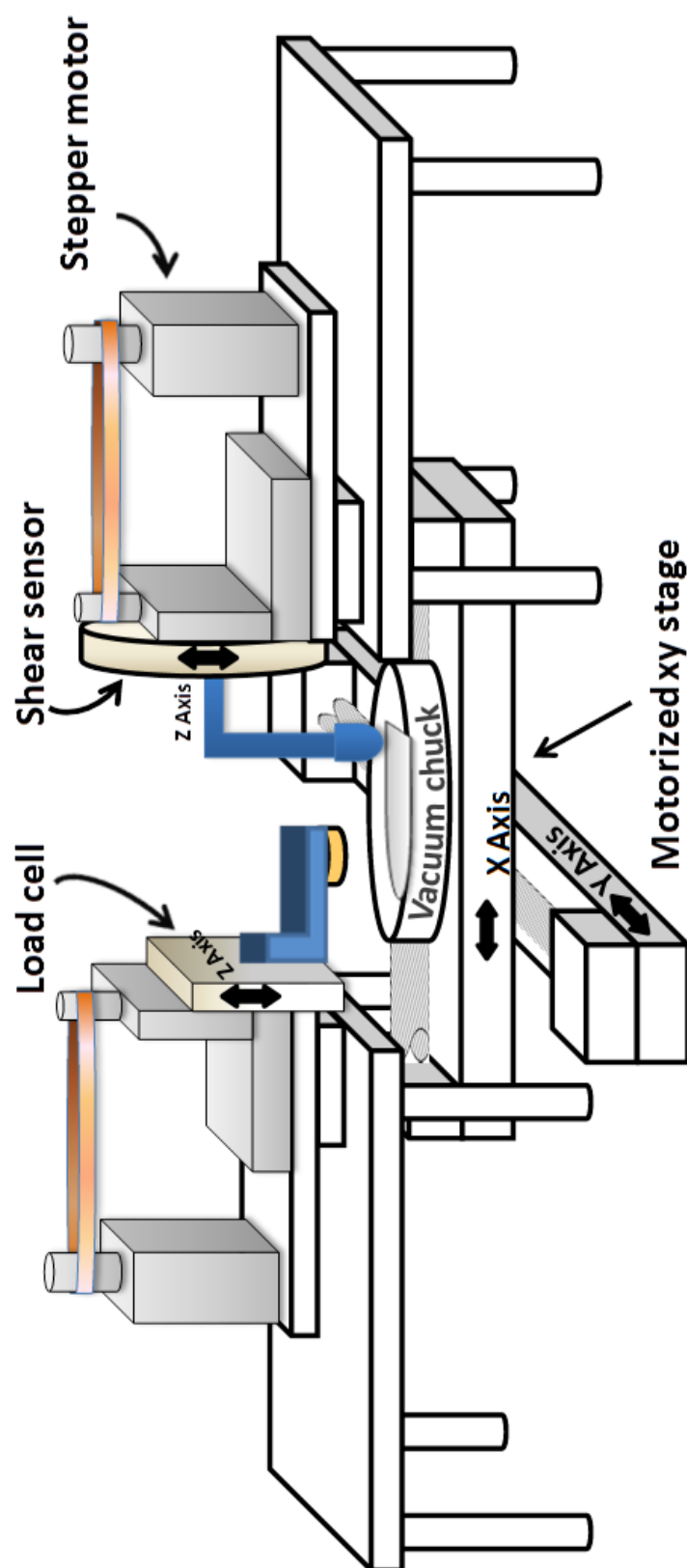


Figure 4.1: Implementation diagram of 3 axis linear stage

Shear and normal forces have individual pressure sensors that are specialized to meet the sensitivity performance requirement.

For an accurate motion control, momentum transfer is employed from horizontal to vertical. A motor induces a horizontal movement ending with vertical force by using mechanical parts within the stepper motor. It is the key to maximize the transfer of horizontal momentum to vertical while avoiding any undesirable vibration caused by momentum transfer when the testing device is in motion. Since the momentum change is dramatic, the supporting part should be rigid enough to endure the perpendicular force on it [14].

The tip of the measurement sensor has a delicate sensor at the end of it. When it stops to measure the normal force with this delicate sensor, it needs to put away all of the linear momentum. It was necessary to deflect any adverse movement by means of having a retarding force which induces the horizontal velocity to become zero. A sudden stop at the end of the tip would cause vibration at the tip that would induce lots of noise on the data. The problem was due to the absence of a physical retarding force to slow down the forward motion, other than the motor control. An effective way to realize the retarding force was providing the slow motion gradient by programming.

For the protection of the device, a clutch mechanism is used with a small torque range to treat a thin and delicate material device. It is important to keep the prototype device safe for several reasons. First of all, the process of making a prototype device takes a long time since it goes through several steps during fabrication under high standard protocol. On the other hand, the number of prototype devices is very limited, since they experience many failures and error correcting steps. To protect the surface of

the sensor, a soft material at the end of the tip acts as the buffer between the tip and the tested GRSC sensor.

Measurement Equipment

The contact tip of each Z axis platform is connected to different types of load sensors. The platform on the left side of the main stage shown in Figure 4.1 is connected to a Digital Force Gage (ZPS-LM-11, Imada), shown in Figure 4.2. The accuracy of the gauge is within a range of $\pm 0.5\% \pm 1$ LSD. The platform on the right side of the main stage shown in Figure 4.1 is connected to the shear force measurement load cell (iLoad-U TUF-002). The example graph of shear force measurement results is shown in Figure 4.3.

Motion of Each Stage

Introduction

To initiate the whole testing process, AutoIt3 was used to enable the process to go from start to end with one button click. The AutoIt3 program managed all of the software applications for measurement equipment, including two load sensors and its software. It also handled the software for controlling the four linear platforms which comprised X, Y, and Z axis stages. To control the four linear stages, low level language code designed by the supplier was used with the bundle program. The whole device has 169 single cells (13x13). Each cell has two detectors placed perpendicular to each other in the X, Y direction. In programming, each row has 13 spots to be measured and there are 13 rows. Measuring shear and normal force is a serial process. The testing proceeds toward a normal pressure measurement process after finishing the entire measurement of the shear force.



Figure 4.2: Normal force sensor gage

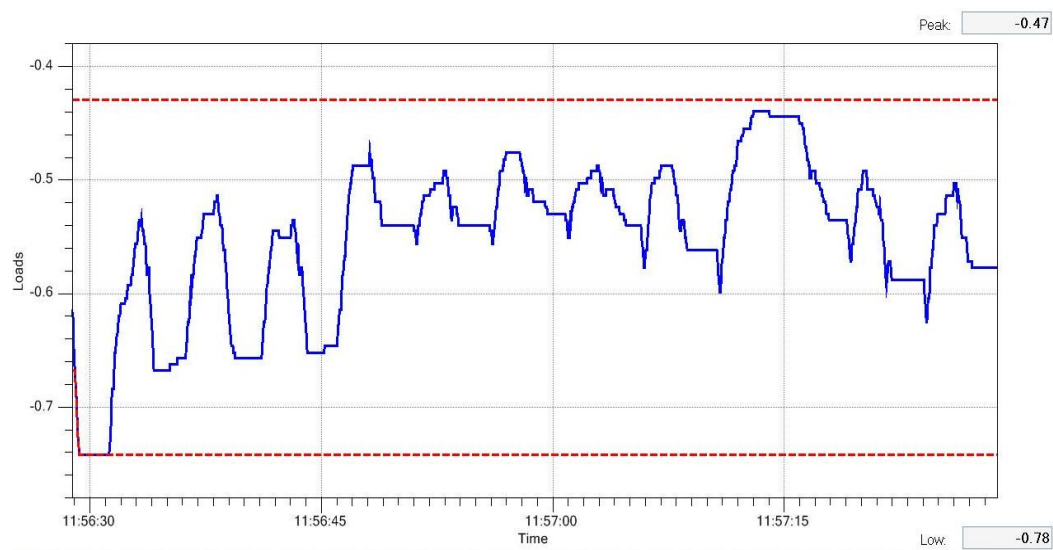


Figure 4.3: Shear force measurement graph

Vertical movement is controlled by a step motor with a timing belt horizontally placed between two pulleys. To measure normal and shear force, two different motorized precision vertical direction platforms were devised at different positions. One is used to measure shear force and the other is for normal force in Z direction. To get the best performance with a microstep driver and motion controller, two NEMA 23 stepper motors are used for two different positions of the z-axis for the sake of high torque at low speed. A four-axis motion controller is used to control all the four axes - x, y, and two z axes - all together at the same time in one program. Figure 4.4 shows the whole testing setup for accuracy testing, including XY linear stages and two z-axis platforms with measurement sensors.

Shear Force Measurement

To measure the shear force, an L-shaped iron probe tip with an elastic material edge was employed. At first, the probe tip moves down and presses the measuring material to different depth according to the amount of force needed to be applied. Second, it moves in a horizontal direction around 1 mm in length to provide a shear pressure on the sensor. After the gauge senses the shear force along with this horizontal movement, the tip is lifted up to the original position. Then, it moves to the next cell. This is one cycle of shear force measurement. This cycle is repeated over a whole sensor area.

Normal Force Measurement

While the L-shaped probe tip has a horizontal movement for shear force measurement, the probe tip does not have horizontal motion for normal force measurement, only vertical. Unlike the shear force measurement, five measurements are

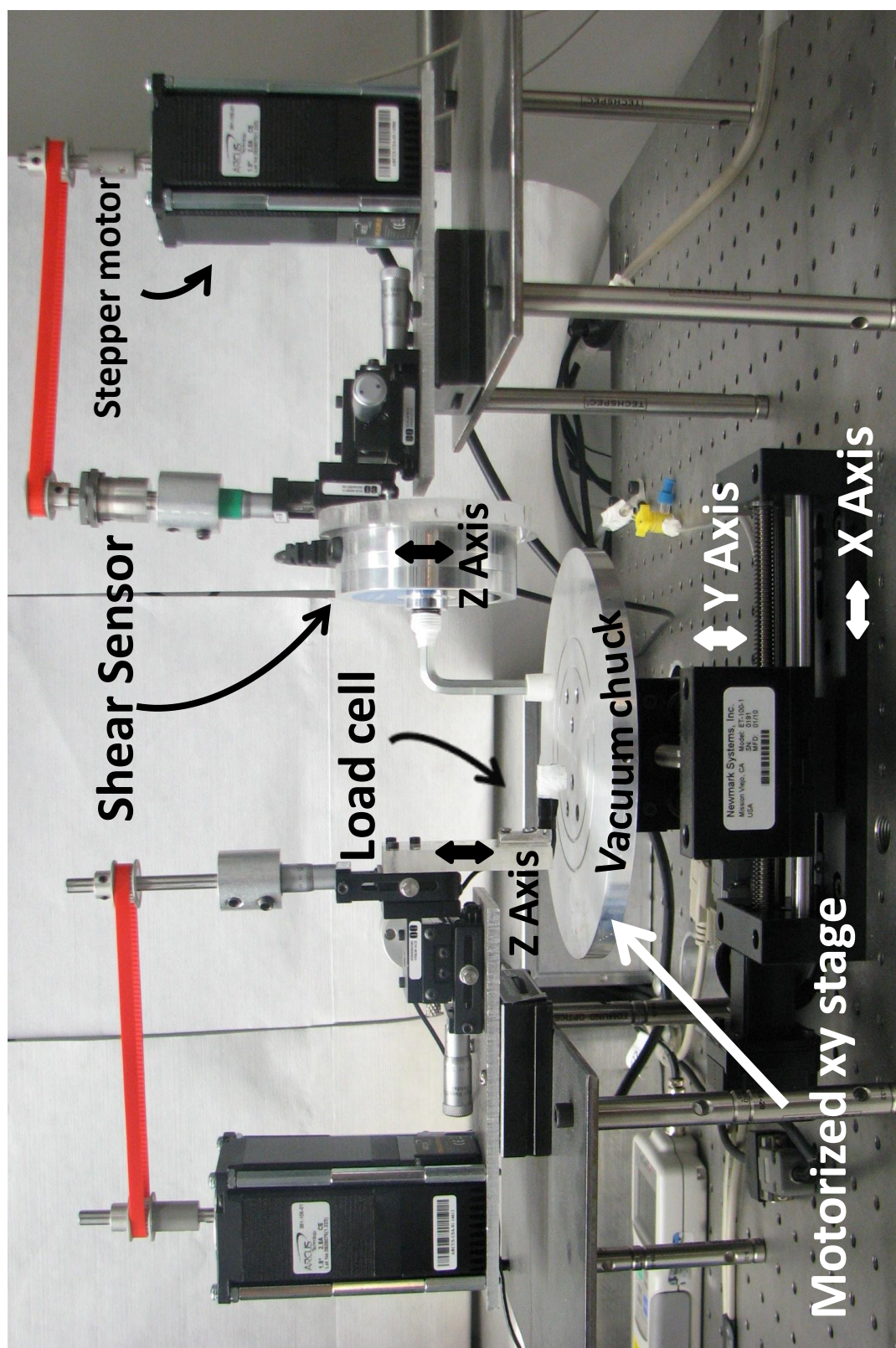


Figure 4.4: Automated 3 axis linear stage for GRSC testing

performed in one cycle. In other words, the tip repeated stopping and moving down five times in one cycle to visualize variation of capacitance with different pressures.

Coarse Testing

The physical testing setup was completed and tested with consecutive movements at every 13x13 spot. There were four axes including the XY stage and two Z axis platforms. The stop and acceleration motion at each spot was smooth, and the tip found the exact position, which should be inside of the 5 x 5 mm² rectangle. After testing the movement of the entire four-axis platform, it is necessary to integrate this physical measurement setting into the rest of the parts; sensor interface, data control, and storage parts which also consist of software and hardware.

Before the integration process, coarse testing was done to the GRSC sensor by manually applying the pressure step by step. An Agilent LCR meter was used to measure the capacitance of the sensor. The calculated value of capacitance with the PDMS thickness 15 µm and overlapping area of 6.1×10⁵µm² is 900 fF.

$$C = \frac{\epsilon_0 \epsilon_r A}{t} = \frac{8.854 \times 10^{12} \times 2.5 \times 6.1 \times 10^5 \times 10^{-12}}{15 \times 10^{-6}} \dots \dots (10)$$

CHAPTER 5

STRESS TESTING

Introduction

The purpose of this test is to check the endurance and survivability of a sensor against numerous external forces during its lifetime. The sensor must stand up to damage and change, which naturally and inevitably occur as a result of long-term use and being exposed to harsh conditions. The reaction of the sensor to external forces could be deformation, bending, torsion, or compression. The most delicate part of the sensor is the liquid conducting wires in the flexible structure. Unless the wires are disconnected or fractured, an effective signal comes out of the output of the sensor and the function of the sensor is still valid. The worst-case result of wear and tear on the sensor is disconnection and fracture of these wires. Coarse testing is enough to see the durability of the sensor. With simple methods, a researcher can determine whether the mechanism of the sensor is well-matched with the expectations of the sensor. For the coarse testing, a U-shaped one line liquid conducting wire is fabricated in the PDMS.

To guarantee sufficient endurance and resistance in real situations for the life of the sensor, the testing environment needs to be harsher than the expected real environments it will face. Bending with a high degree is one of the most extreme external forces which the sensor could experience. Since the sensor will be implanted in the insole of the shoe, there are not many chances that the shoe will bend to a high degree. Another

possibility of sensor damage is penetration of a foreign object. Again, because the sensor is placed in the shoe insole, it is not a normal outcome. The number of cycles of testing must be adequate to check the requirements as mentioned above.

Data Control

Physical Blocks and Peripheral Connection

There are three big physical blocks for the testing setup structure – physical stage, data interface, and the PC. The physical stage consists of the sample stage and the actuation part. The sample stage holds the flexible liquid channel sample securely, and it also determines the length of the channel, which touches to the metal lever on the actuation part. In turn, it determines the bending angle of the flexible liquid channel. The actuation part actuates the pushing motion after receiving the data from a relay I/O interface. The data interface setup has a digital multimeter, a relay I/O interface. The PC is the brain of this whole system that controls all the behavior of the system (Multimeter and motors) and deals with information gathering (sensor) and memory.

There are two main functions of the PC when communicating with devices. First is sending and receiving the command line input and output from the PC to the devices. Second is receiving the data and saving it in real time. Visual Basic with .Net script was used to control the whole setup. The PC is linked with the multimeter and I/O interface. At first, the PC sends the command to the I/O interface and positions the metal lever to push the flexible liquid channel up and down. Once the liquid metal channel gets to the desired position, the PC sends the command to the multimeter to read a resistance and these data are sent back to the PC through the multimeter and stored in the correct format.

The key in this data flow, as shown in Figure 5.1, is not only integrating all the devices but synchronizing a single set of data between these devices, automatically exchanging the data, and copying them into a correct place in the correct format. It should behave like one body with one head without any collision between them. A small failure could ruin the whole testing procedure. The failure here includes not only data communication conflict but also physical malfunctions as well. The actuation movement is a regular but periodic movement.

An incorrect command from data communication conflict or unexpected external forces could cause nonperiodic or irregular action. This could damage the physical structure of the device.

Effort should be made to prevent this failure. However, it is extremely difficult to make zero errors during the test, and this kind of repetitive testing could be tremendously affected by one error. An alternative way to make the testing work is that the failure could be assumed to happen in a certain amount of time. In this case, making a checkpoint in between the cycle could handle unexpected errors. Real time data saving to secure data storage is also helpful. All these failure handling methods were applied in this system, as you see in scripts which are appended at the end of this chapter.

Programming

To communicate with the multimeter, the Standard Commands for Programmable Instruments (SCPI) is used with an IVI driver for the test and measurement instruments. SCPI has a hierarchical structure, also known as a tree system. This defines a group of commands to control instruments which use ASCII characters, providing some basic

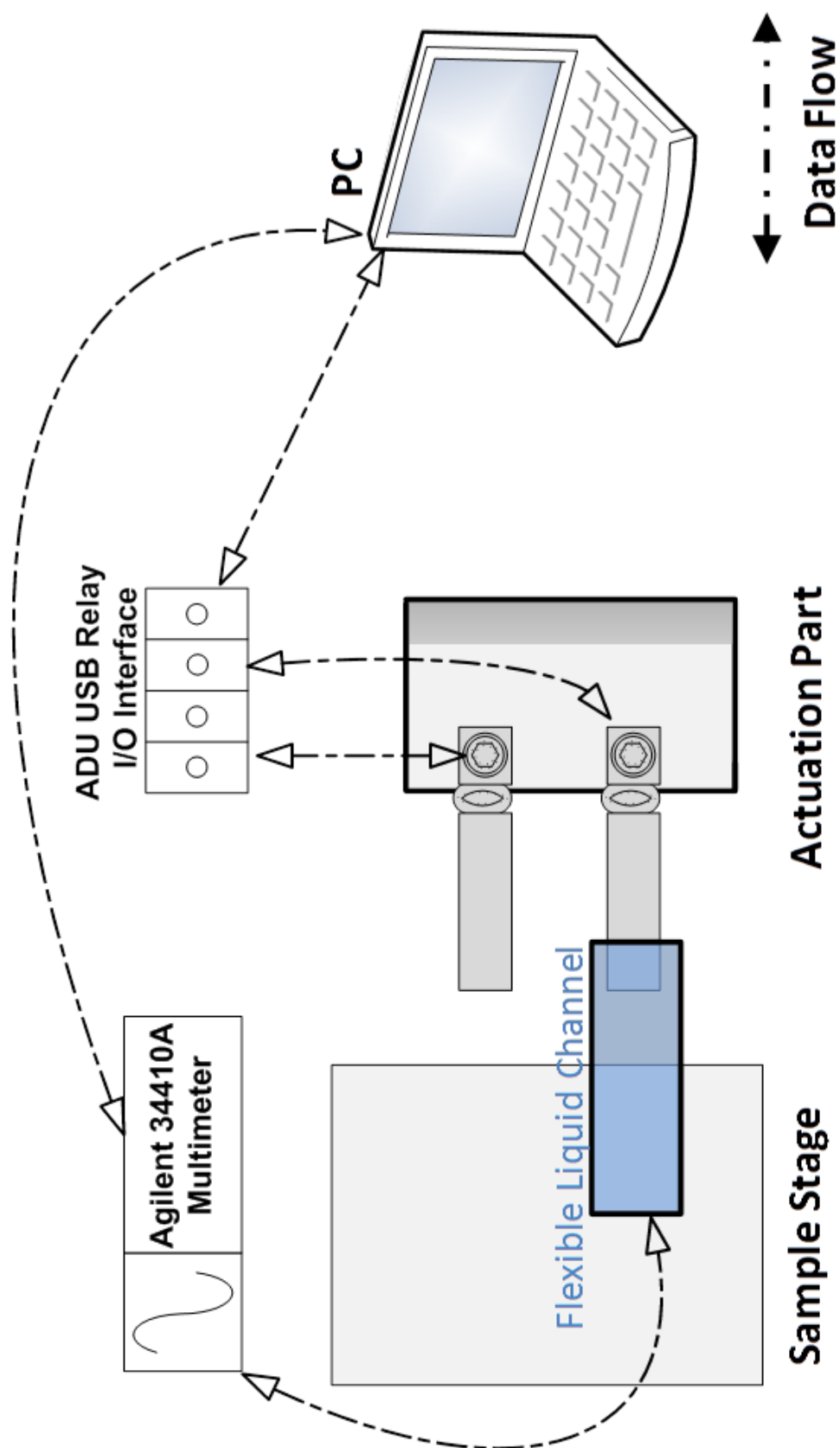


Figure 5.1: Data flow diagram

standardization and consistency to the commands. For example, when you specify the resolution of voltage, the SCPI command is “CONF:VOLT:DC 10,0.001,” which specifies the resolution 4 1/2 digits on the 10 V-dc range.

SCPI itself, however, creates and sends the instrument the ASCII syntax, then reads back a string, and builds it into a variable. To simplify these processes, a driver could be used by calling a function and passing a variable to it to return the desired value. By using a driver, it is no longer necessary to hunt around the programming guide to find the right SCPI command and exact syntax. The shortcoming and issue of using a driver in various kinds of instruments is the inconsistency across instruments produced by different vendors. To solve this problem and improve the usage of the driver, a consortium called the Interchangeable Virtual Instruments (IVI) Foundation was made. The IVI Foundation has created IVI class specifications that define the capabilities for drivers for certain number of instrument classes. This gives better performance, cuts the cost of development, and makes interchangeability easier. By utilizing this interchangeability, various instruments could be linked together and controlled by one place.

Strong support for COM components was integrated in the .NET environment by Microsoft. The .NET API (Application Programming Interface) takes advantage of most IVI-COM drivers, which is supported from the provider. The API environment is useful for adding additional functionality to the executable driver and creating a set of standards.

Testing Equipment

Figure 5.2 depicts the main parts of the hardware which are the sample stage and actuation part. Hardware for the stress setup consists of an actuation stage, a digital

multimeter, a relay I/O interface, and a fixed stage for the sample, as shown in Figure 5.3.

The actuation stage includes two linear solenoid actuators, two metal levers, and supporting parts. Rigid support of the piston actuator is fundamental for several hundred thousand cycles of testing for a couple of days without any break. The touching point of the metal lever on the liquid metal channel determines the bending angle of the channel. The steeper the bending angle, the stronger the bending pressure that is applied on the channel.

The pushing force was actuated by a linear solenoid piston. It creates linear motion simply and economically. A problem with this setup is that the pushing distance is too short to bend the sensor to a high degree. It pushes only 12.7 mm with a light load. To compensate for this problem, a metal lever is employed to multiply the pushing distance. The length of the lever is 101.6 mm, and the piston is placed 12.7 mm from the end of the lever. Mathematically, the traveling distance at the end of the lever should be 101.6 mm, with a light load. However, the pushing distance is only 50.8 mm because of the lack of enough pushing force of the solenoid piston and the resistance force (load).

Data Analysis

The sensor was still working after 700 thousand testing cycles, which could guarantee not only the endurance of the testing device, but also of the testing setup of it. As shown in Figure 5.4, the measured resistance was about 20 Ω , yielding a resistivity of $0.75 \times 10^{-6} \Omega\text{-m}$. The sample was periodically stressed with a ~40% strain while the resistance of the line was recorded using a multimeter.

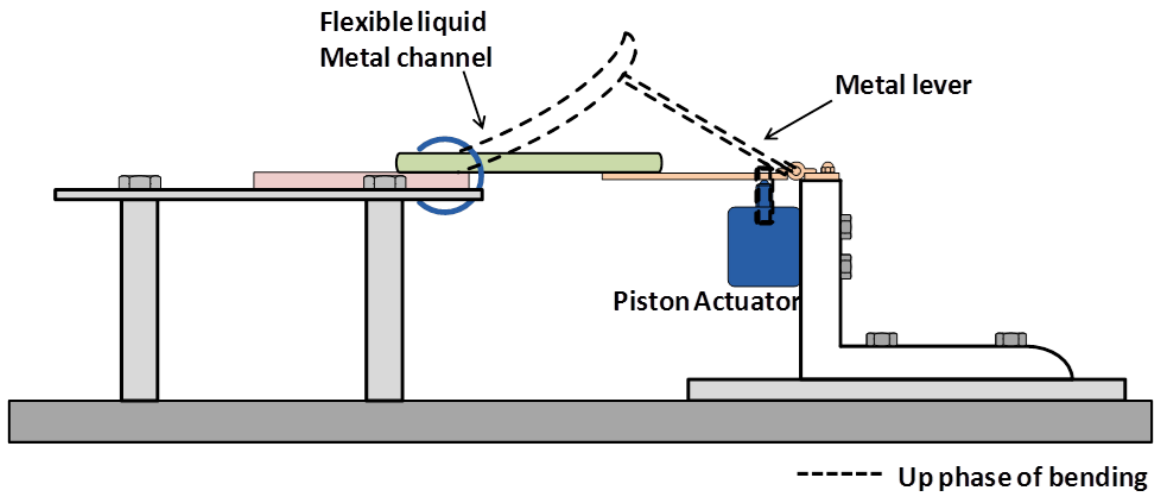


Figure 5.2: Stress testing setup

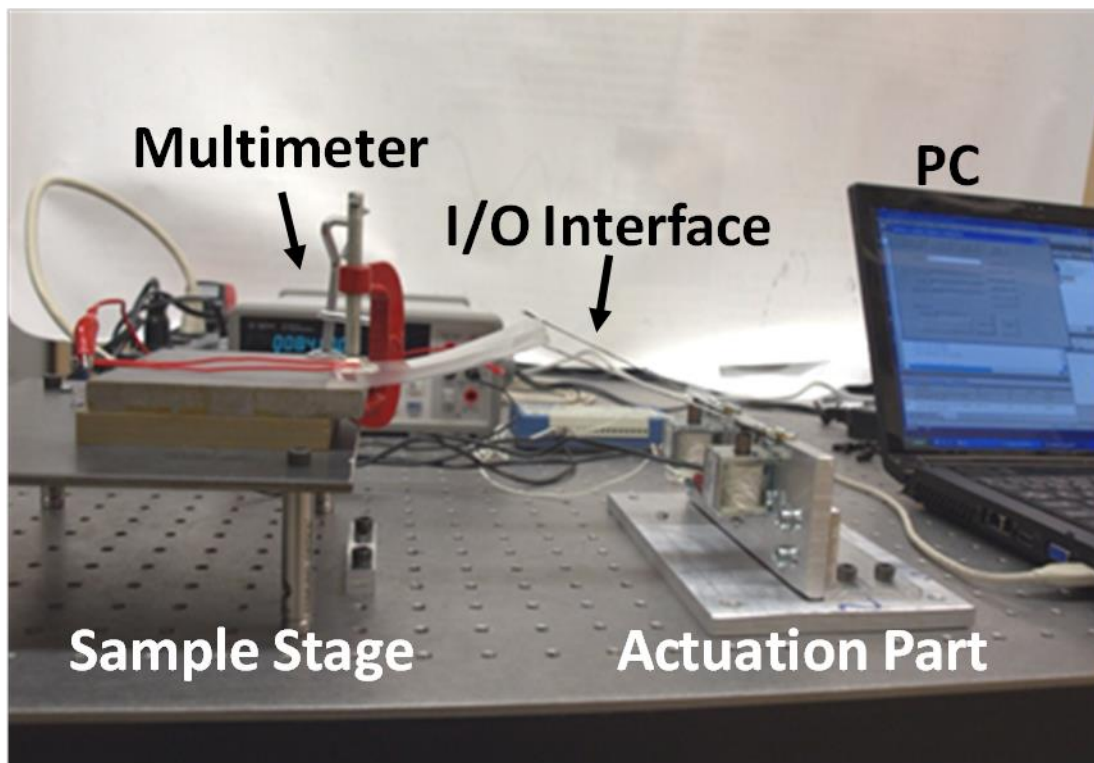


Figure 5.3: Realization of stress testing setup

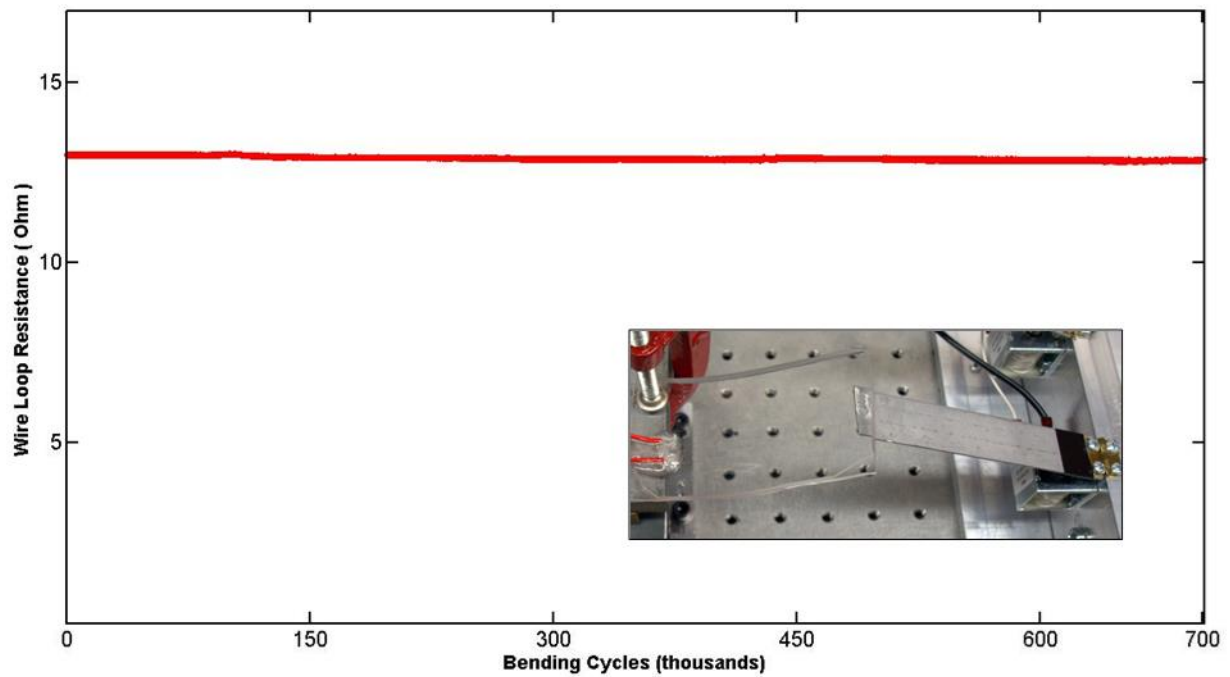


Figure 5.4: Reliability of wire under a very large number of bending cycles

The ten sets of up-and-down pairs were sampled and displayed in Figure 5.5 and Table 5.1. They show the numerical values: the max value is 12.89Ω and min value is 12.85 , so the resistance value is pretty consistent.

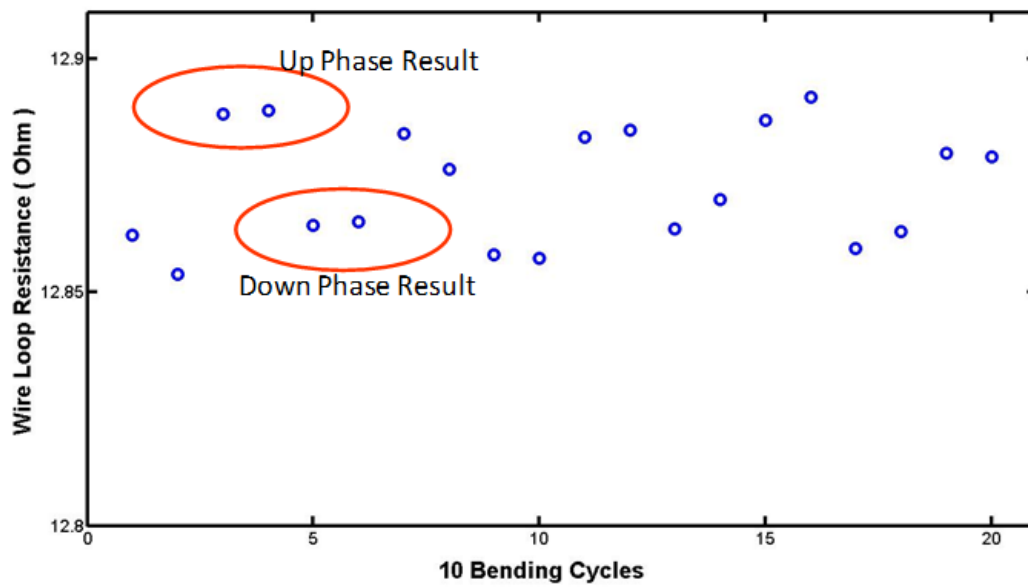


Figure 5.5: Ten pairs of sample cycles

Table 5.1 Ten pairs of sampled values

	1st	2nd
down	12.86221	12.85378
up	12.88821	12.88891
down	12.86432	12.86502
up	12.88399	12.87627
down	12.858	12.8573
up	12.88329	12.8847
down	12.86362	12.86994
up	12.8868	12.89172
down	12.8594	12.86292
up	12.87978	12.87908

CHAPTER 6

INTEGRATION AND AUTOMATION

Introduction

A software application is absolutely essential for testing, not only to control the equipment but also to collect and analyze the data. In this project, there are four individual linear platforms, and to control these platforms, one control program is used. Two load sensors also have their individual programs to log and analyze the data. The difficult part of the testing aspect was that a single GRSC pressure sensor has 169 single cells to be measured. By maximizing testing benefits, the whole timeline can be shortened and the cost reduced. However, controlling a bunch of physical equipment and software applications at the same time does not simply maximize the testing benefits and fulfill the whole testing purpose.

In general testing, the same task is running repeatedly in the same manner, which means that the task takes place with the same amount of time while different kinds of constant variables are applied. The variable factor could be modified, but a critical issue, especially for testing, is that a changing variable should be systematic in terms of duration, period, magnitude, and characteristic of the variable. When a variable is changing, keeping the environment the same all the time is mandatory. These testing requirements end up with the key concept and benefit of automation.

Automating the whole process was most important in this testing. To achieve productivity, planning a good strategy is the necessary groundwork before realizing automation. Another important point in automation is searching for a useful method and technology that fits the purpose of the project [15]. It is required to verify each technical element including software, hardware, and research instruments, and find the connection between each element and the data flow from one to another. Even if one factor of the technology is strong, if it is not mixed up well and does not harmonize, then the method cannot achieve productivity or efficiency. All quality control, testing, and analytical processes are directly related with this integration issue [16].

Integration is the procedure of how to collect and put a set of elements all together in an efficient and valid way. In a laboratory environment, integration in an organized way could reduce the time and effort of automation.

Physical Setup Movement Control

The object of automation in this project could be divided into two parts. One is physical setting movement control, and the other is data control. In the previous chapter, we discussed the physical testing setup for 3-axis movements. That includes what was built in the testing setup, how those were built, and how they move.

To control the movement of each linear stage, low level language code designed by the supplier was used with the bundle program. Each linear stage position was directly designated by this code, and the form of the code is straightforward. This code could define all the detail parameters of the linear stage movement, including all the maximum and minimum acceleration and speed, x, y, z position, and transition time as well.

The next step was joining this program with other windows-based application tools, which were mostly sensor applications for automating administrative tasks. In the system administration area, AutoIt was used to control all the applications in the Windows environment. The strong advantage of RunAs support of Autoit is that unattended installation and configuration changes could be performed. While the tip of the pressure sensor at the end of the platform was changing, the application of the pressure sensor should be simultaneously controlled, as shown in Figure 6.1.

Data Control

Overall Data Flow

As mentioned before, the whole data control structure is shown in Figure 6.2. The sensor interface board accepts a TTL address input from the I/O interface to electronically select the sensor site. The sensor interface board is controlled by a 7-bit address. The 7-bit includes a 4-bit row address and 3-bit column address. One more extra bit is determined by channel selection. The total number of bits which selects the GRSC pressure pad site is eight.

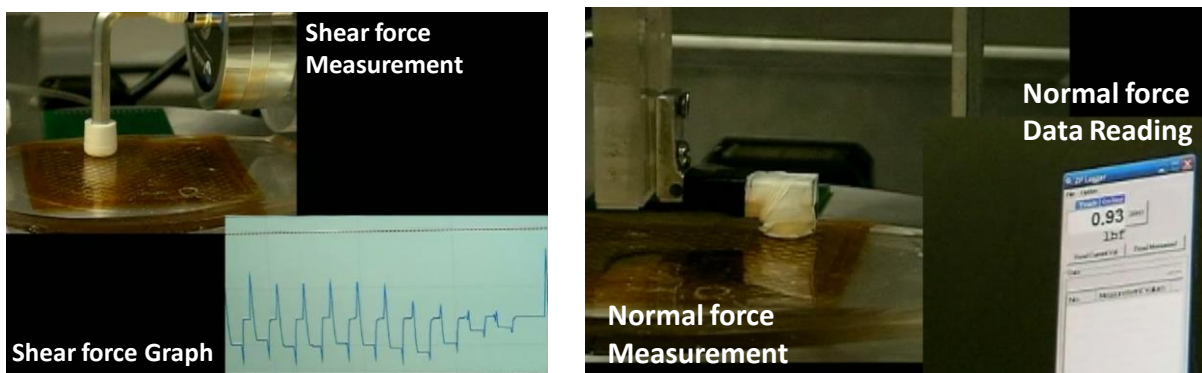


Figure 6.1: Normal and shear force measurement

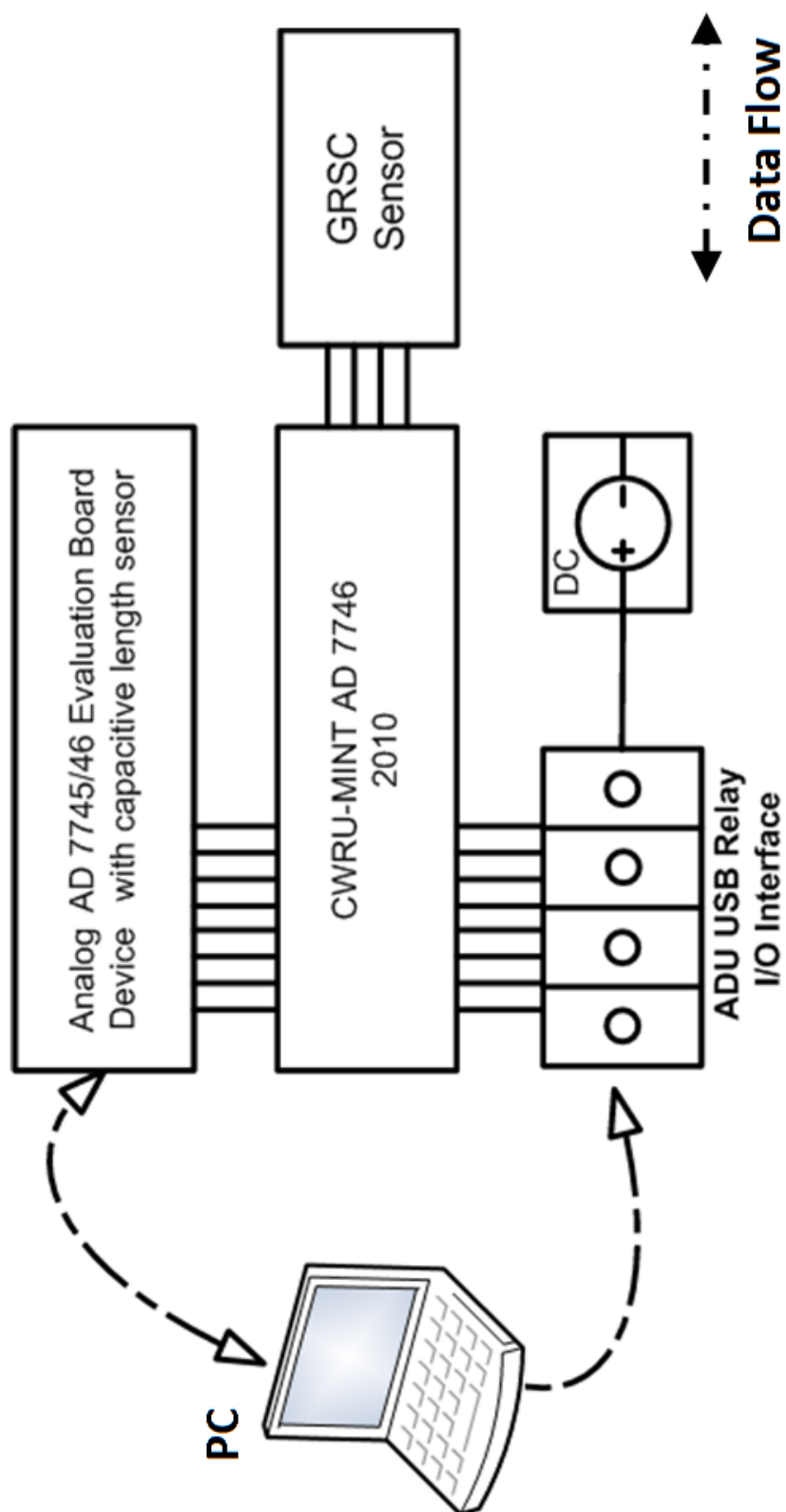


Figure 6.2: Data control structure diagram

When a TTL signal is given to the board, it changes the address of the on-board multiplexers that control which row and column is connected to the C/V. The MUX part numbers are labeled on the PCB and they are AD 6706 and MAX4051A.

For shear sensing, the circuits were designed to handle from about 1 – 10 % capacitance value change based on a 1pF nominal capacitance value. Since the sensor is not a fully differential structure for the Z-axis sensing, an average capacitance value throughout the entire array is used as the reference capacitor. The variation of the capacitance values from the array is critical. The circuits were designed to handle up to a 10% Z-axis capacitance values change for a nominal value of 2 pF (two half sensors connected in parallel) due to an applied pressure.

This interface board is linked with ADI Eval software through an AD 7746 evaluation board to record capacitance and select input channel. These boards are depicted in Figure 6.3. For normal pressure measurement, a pressure pad was characterized cell-by-cell.

However, the software that comes with the board displays the capacitance, but cannot fetch the reading from the screen. Another issue was to keep tracking the row and column information of the cell on the GRSC sensor. If the cell spot information is missing among 169 spots, it is difficult to map the capacitance on the GRSC sensor and calculate the acceleration. Row and column information are inputs to the board. The problem is that the board does not keep the row and column information on the output data. Therefore, position information needs to be stored for a while and matched with output capacitance data when it comes out of the evaluation board.

First, how to get the necessary data is an issue here. USB software was used to

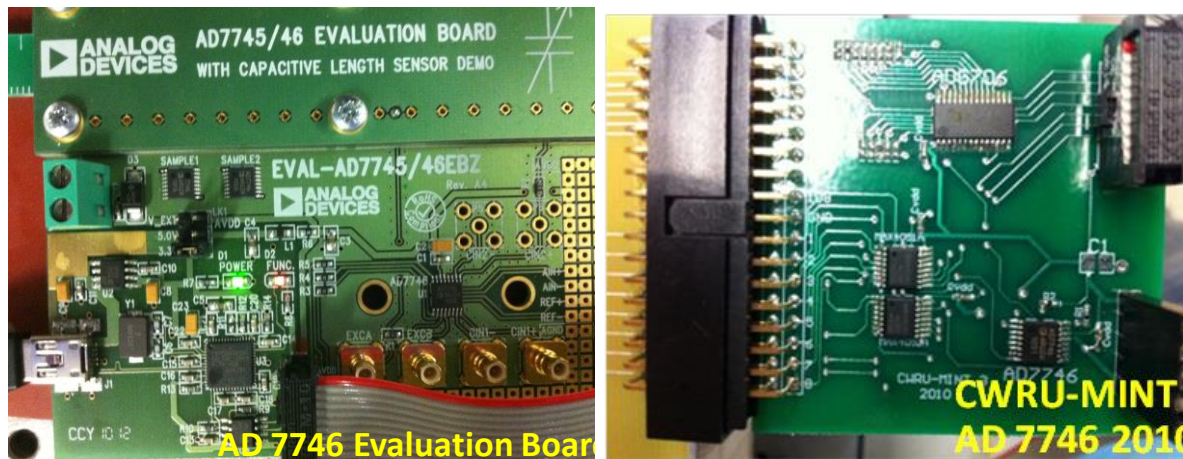


Figure 6.3: AD 7746 evaluation and MINT-CV-M1 extension board²

fetch off the capacitance value. This USB software is monitoring the data traffic through a USB cable connecting the evaluation board to the PC. To be able to recognize a valid data pattern in the USB data stream, the pattern of the AD7746 registers was referred from register descriptions in the chip datasheet, and the correct pattern was captured from the USB data stream. Consecutive raw data in the series were captured from the software and the normal force data were recorded from the IMADA software. The raw data, for instance "02 01 88 A6 00 00 00," were converted to a valid capacitance form. At the end, an index of one position is getting valid information: one is capacitance and the other is pressure.

The sensor location address table was stored in an Excel data sheet, and the address from the table was directly sent to the TTL board, which in turn linked to the interface board. A programming routine was required to fetch this number off the board and match the capacitance value with position information. Position information is sent to

² the AD 7746 Evaluation Board and the CWRU-MINT Extension Board were contributed by Michel Sister from CWRU

the I/O interface from the Excel table, and stored in the memory until it meets to output capacitance data. Raw capacitance data are captured from the USB data traffic and converted to the desired capacitance data. Pressure measurement is simultaneously done by the sensor and stored to software. It is directly transferred to a final database to match with position information and capacitance on the position. The Visual Basic .Net programming routine took a leading role to connect all the data flow and manipulation and integrate it into one data form.

Device Communication and Visual Basic .Net

Device communication is at the heart of engineering laboratory applications and one of the significant functions done by computers. Device communication includes reading a measurement from a sensor, collecting data from a data acquisition board, transmitting data to a remote computer, or sending commands to a remotely controlled device. Visual Basic .Net gives many ways to communicate to devices and run software programs on the same machine which are connected through cable or network [17].

A .Net application can contain more than one assembly, which is an individual EXE or DLL executable file. Since the .NET object hierarchy has all the objects which could be manipulated in any .NET language, a degree of cross-language interoperability is achieved. For instance, an interface with Visual Basic can be made and a C++ class can be implemented in it. It is compatible with COM-based languages as well. This characteristic helped us to choose and utilize the .Net environment to realize this testing system.

The difficult parts in data communication were extracting data from an Excel file, correctly conveying it to the system, and saving the data into it. Dynamic Data Exchange

(DDE) was applied to exchange the data from Excel to the other Windows application.

The destination application could establish a channel by specifying the source application name, the topic of conversation, and the data item. Figure 6.4 shows a total control terminal for normal and shear force measurement, and an example code for DDE is shown in Figure 6.5.

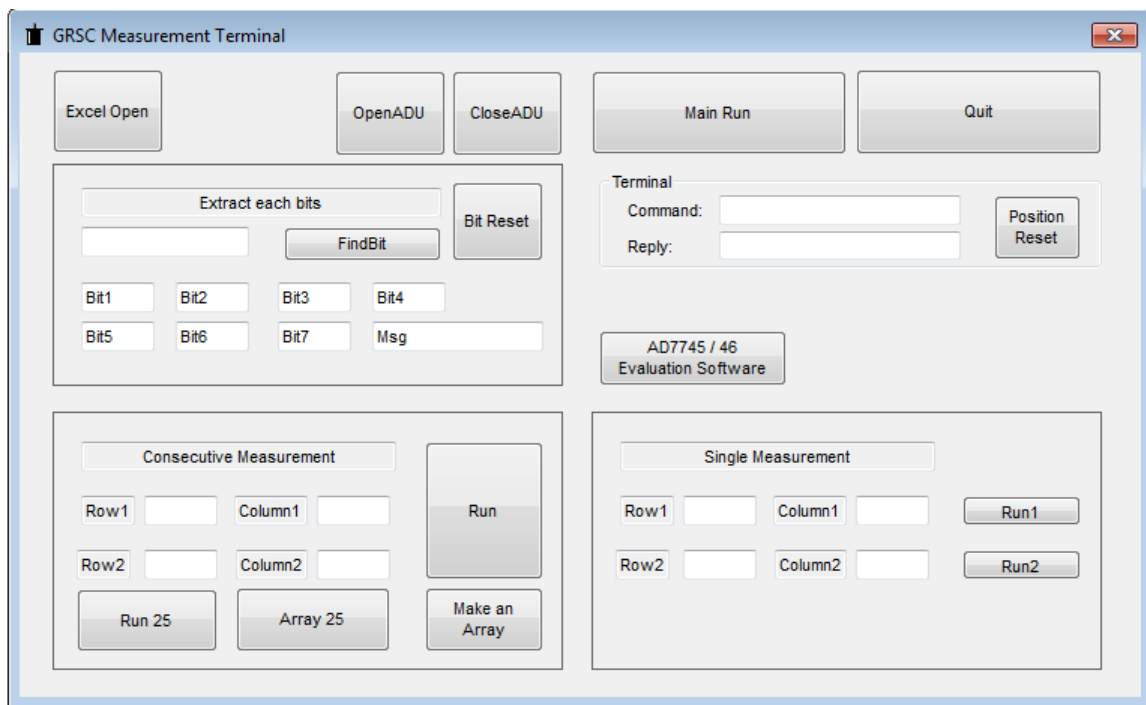


Figure 6.4: User interface control terminal

```

Dim oExcel As Application = CreateObject("Excel.Application")

Dim oBook As Workbook =

oExcel.Workbooks.Open("F:\Data\UBSlyzer\test.csv",
[ReadOnly]:=True)

Dim oSheet As Worksheet = oBook.Worksheets("test")

oSheet.Select()

oExcel.DisplayAlerts = False

```

Figure 6.5 Sample code for DDE

CHAPTER 7

DATA ANALYSIS AND CONCLUSION

Data Analysis

The array data with the slow scanning setup is shown in Figure 7.1 and 7.2. Figure 7.1 depicts that the parasitic capacitance accommodates 2.0-2.5 pF on the sensor fabricated without a PDMS layer. On the other hand, the sensor array with a PDMS layer has a capacitance readout in the range of 3.0 - 3.5 pF, as shown in Figure 7.2. Therefore, the capacitance per sensor set of four is about 1pF, and each set of sensor elements provides 0.25pF.

After obtaining the reference capacitance from the sensor array with and without a PDMS layer, a multiple of 0.8 pound weights were applied on the sensor. Before applying the weight, the pressure distribution showed an even configuration on the whole surface of the sensor. Once a 0.8 lb weight was placed on the sensor array, the spot where the weight was on turned to red, as shown in Figure 7.3. After measuring one weight, more weights were added on top of the previous weights step by step. Figure 7.4 and 7.5 depict the diagram when the different number of 0.8 lb weights was applied on the sensor array.

The average value after subtracting the reference is 0.189 lb at the first one, and the second measurement value after adding one more 0.8 lb weight is 0.209 lb.

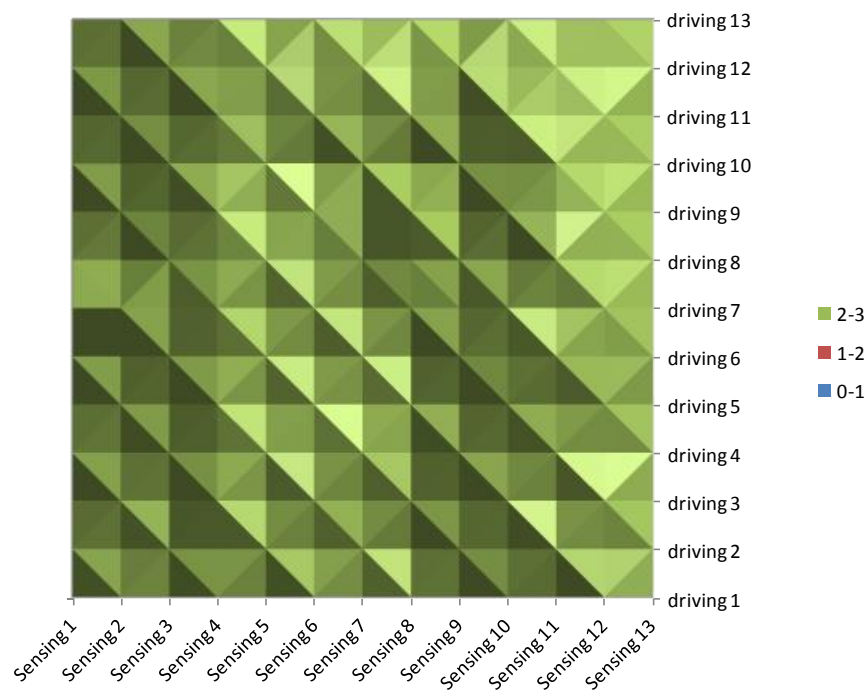


Figure 7.1: Reference measurement without PDMS

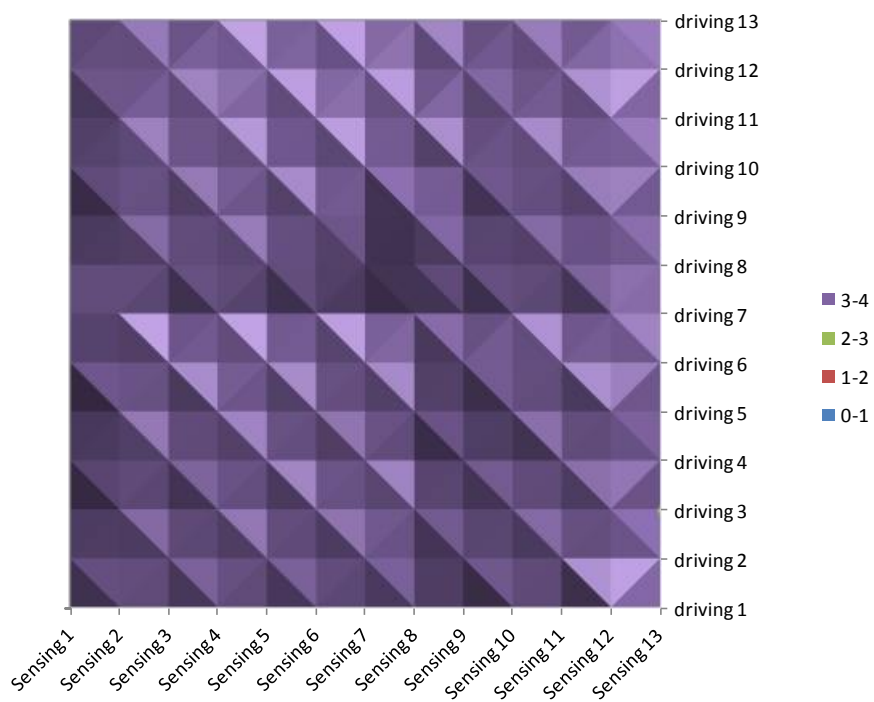


Figure 7.2: Reference measurement with PDMS

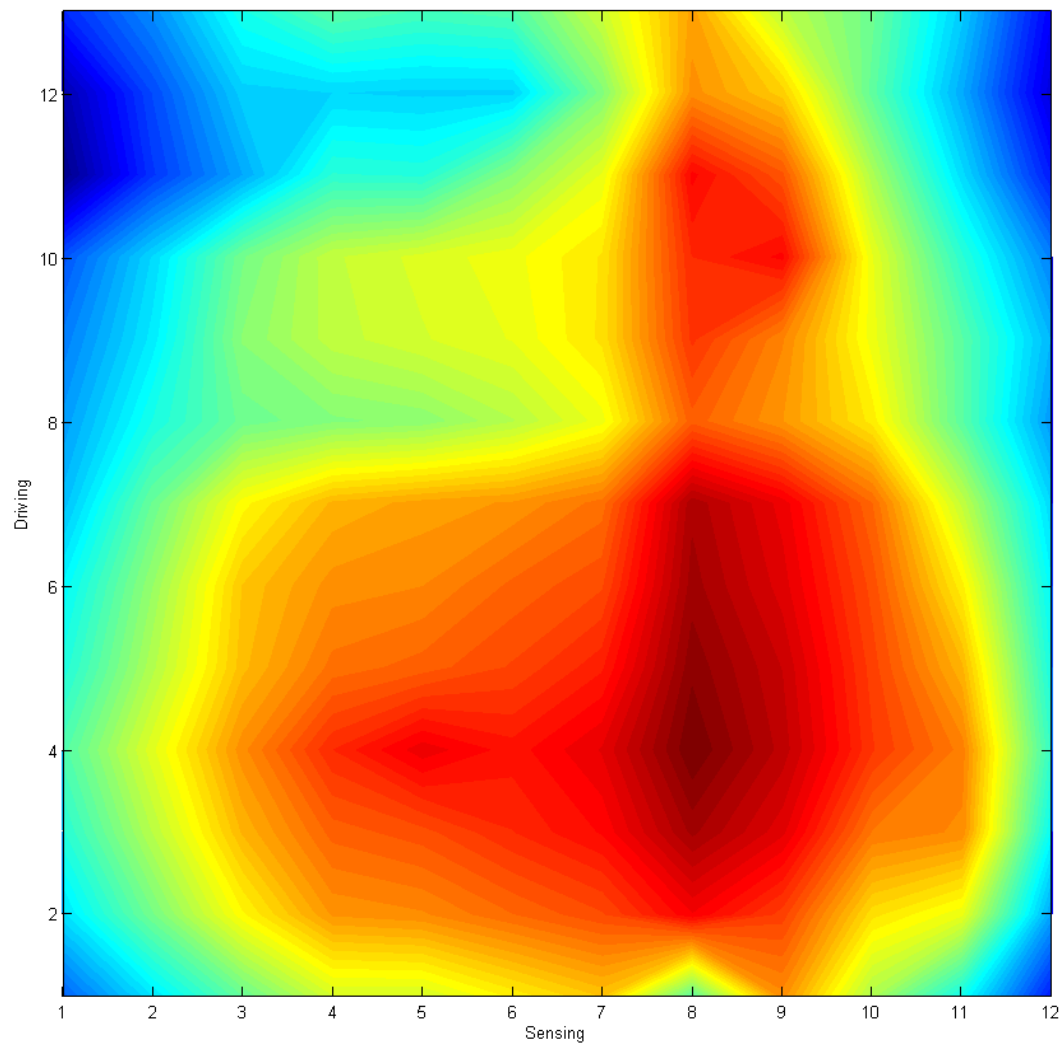


Figure 7.3: Mapping with 0.8 lb weight

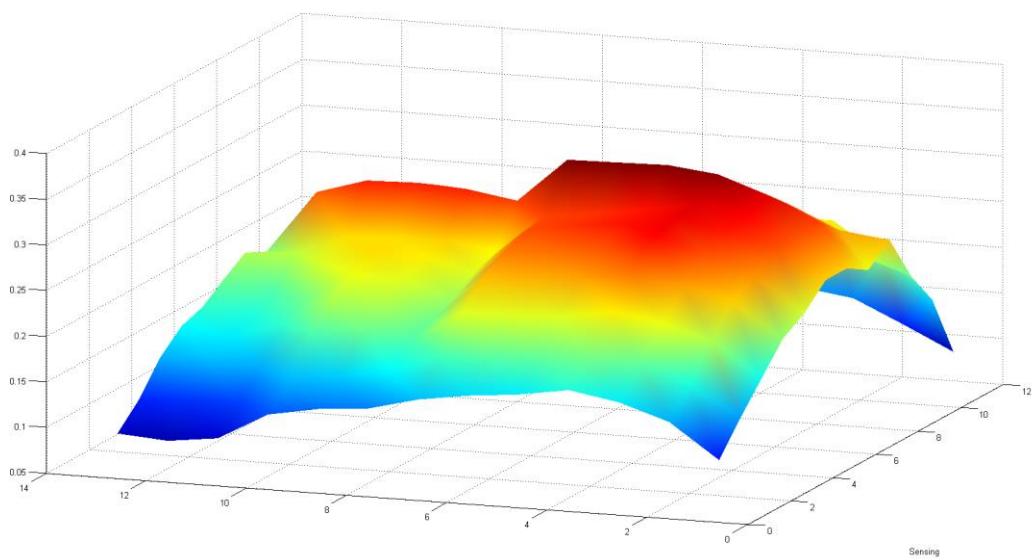


Figure 7.4: Mapping with three weights

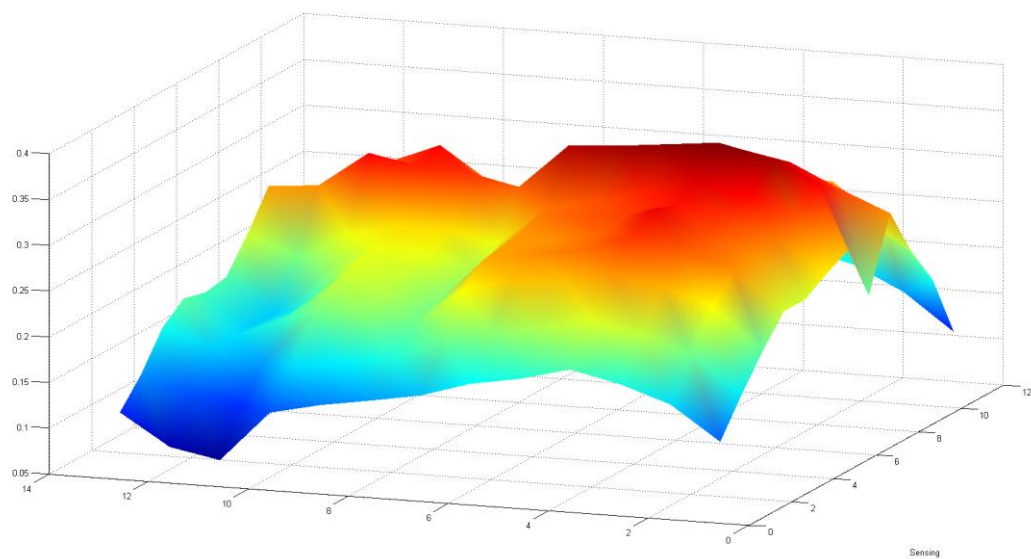


Figure 7.5: Mapping with six weights

Conclusion

In this project, we developed a pressure-sensor testing setup and tested a pressure pad fabricated in our research group. Slow scanning can detect the pressure changes, and all the data can be stored in real time. Stress testing results show that GRSC sensor lines are intact and continuous even after 600,000 cycles of large strain deformation. The goal for the next step is sweeping the array and performing the conversion of capacitance to pressure and shear through a calibration table. Measuring shear force in a fast scanning setup is another issue in the future.

There should also be standards for systems development, and those standards should reflect the current state-of-the-art technologies. The process can detect flaws in a system, missing components, and inconsistencies before the actual development process begins, saving time, money, frustration, and yielding a better product. Periodic checks of systems and networks are necessary.

APPENDIX

SAMPLE CODE OF VISUAL BASIC .NET FOR STRESS TESTING

Sample Code of Visual Basic .NET for Stress Testing

```

OptionStrictOff
OptionExplicitOn
Imports System
Imports System.IO
Imports System.Text
Imports System.Collections.Generic

FriendClass Form1
Inherits System.Windows.Forms.Form
Private ioDmm As Ivi.Visa.Interop.FormattedIO488
Dim aduHandle AsInteger
DeclareSub Sleep Lib "kernel32" Alias "Sleep" (ByVal dwMilliseconds AsLong)

PrivateSub Close_Renamed_Click(ByVal eventSender As System.Object, ByVal eventArgs As
System.EventArgs) Handles Close_Renamed.Click
    CloseAduDevice(aduHandle)
EndSub
PrivateSub Open_Click(ByVal eventSender As System.Object, ByVal eventArgs As
System.EventArgs) Handles Open.Click
    aduHandle = OpenAduDevice(1)
EndSub
PrivateSub btnInitIO_Click(ByVal sender As System.Object, ByVal e As System.EventArgs) Handles
btnInitIO.Click
Dim mgr As Ivi.Visa.Interop.ResourceManager
Dim ioAddress AsString
OnErrorGoTo ioError
    ioAddress = txtAddress.Text
    txtAddress.Text = ioAddress
    mgr = New Ivi.Visa.Interop.ResourceManager
    ioDmm = New Ivi.Visa.Interop.FormattedIO488
    ioDmm.IO() = mgr.Open(ioAddress)
    MULTEnableCtrl(True)

```

ExitSub

ioError:

MsgBox("InitIO Error:" & vbCrLf & Err.Description)

EndSub

PrivateSub btnClose_Click(ByVal sender As System.Object, ByVal e As System.EventArgs) Handles

btnClose.Click

ioDmm.IO.Close()

MULTEnableCtrl(False)

EndSub

-
-
-

PrivateSub CombinedRun_Click(ByVal sender As System.Object, ByVal e As System.EventArgs)

Handles CombinedRun.Click

Dim Readings()

Dim iRC As Integer

Dim i As Integer

OnErrorGoTo ioError

For i = 1 To 1000000 Step 1

iRC = WriteAduDevice(aduHandle, "sk0", 4, 0, 500)

Sleep(250)

With ioDmm

.WriteString(":CONF:RES 10, 0.001")

.WriteString("SAMP:COUN 1")

.WriteString("Read?")

EndWith

Readings = ioDmm.ReadList

txtReading1.Text = Readings(0)

Using theWriter AsNew IO.StreamWriter("out.txt", True)

ForEach currentitem AsStringIn Readings

theWriter.WriteLine(currentitem)

Next

EndUsing

```

iRC = WriteAduDevice(aduHandle, "rk0", 4, 0, 500)
Sleep(250)
With ioDmm
    .WriteString(":CONF:RES 10, 0.001")
    .WriteString("SAMP:COUN 1")
    .WriteString("Read?")
EndWith
Readings = ioDmm.ReadList
txtReading1.Text = Readings(0)
Using theWriter AsNew IO.StreamWriter("out.txt", True)
ForEach currentitem AsStringIn Readings
    theWriter.WriteLine(currentitem)
Next
EndUsing
Next i
ExitSub
ioError:
    MsgBox("Error Getting Readings:" & vbCrLf & Err.Description)
EndSub
PrivateSub txtToDisplay_TextChanged(ByVal sender As System.Object, ByVal e As
System.EventArgs) Handles txtToDisplay.TextChanged
EndSub
EndClass

```

REFERENCES

- [1] H. M. Schepers, H. F. J. M. Koopman, and P. H. Veltink, "Ambulatory assessment of ankle and foot dynamics," *Ieee Transactions on Biomedical Engineering*, vol. 54, pp. 895-902, May 2007.
- [2] D. Roetenberg, P. J. Slycke, and P. H. Veltink, "Ambulatory Position and Orientation Tracking Fusing Magnetic and Inertial Sensing," *Biomedical Engineering, IEEE Transactions on*, vol. 54, pp. 883-890, 2007.
- [3] I. Skog and P. Handel, "In-Car Positioning and Navigation Technologies-A Survey," *Ieee Transactions on Intelligent Transportation Systems*, vol. 10, pp. 4-21, Mar 2009.
- [4] X. N. NASER EL-SHEIMY. (2007) The promise of MEMS to the navigation community. *InsideGNSS*. 11. Available: <http://www.insidegnss.com/auto/IG0307el-sheimyFinal.pdf>
- [5] A. M. Sabatini, "Quaternion-based extended Kalman filter for determining orientation by inertial and magnetic sensing," *Ieee Transactions on Biomedical Engineering*, vol. 53, pp. 1346-1356, Jul 2006.
- [6] I. Skog, P. Handel, J. O. Nilsson, and J. Rantakokko, "Zero-Velocity Detection- An Algorithm Evaluation," *Ieee Transactions on Biomedical Engineering*, vol. 57, pp. 2657-2666, Nov 2010.
- [7] C. Randell, C. Djiallis, and H. Muller, "Personal position measurement using dead reckoning," in *Wearable Computers, 2003. Proceedings. Seventh IEEE International Symposium on*, 2003, pp. 166-173.
- [8] N. Bowditch and United States. National Imagery and Mapping Agency., *The American practical navigator : an epitome of navigation*, 2002 bicentennial ed. Bethesda, MD
- [9] M. H. Lee and H. R. Nicholls, "Review Article Tactile sensing for mechatronics—a state of the art survey," *Mechatronics*, vol. 9, pp. 1-31, 2/1/ 1999.
- [10] J. G. L.-M. Rocha, Senentxu, *Sensors: Focus on Tactile Force and Stress Sensors*. Vienna: In Tech, 2008.
- [11] J. E. Mark, *Polymer Data Handbook*: Oxford University Press, USA, 2009.
- [12] K. B. Shimoga and A. A. Goldenberg, "Soft materials for robotic fingers," in *Robotics and Automation, 1992. Proceedings., 1992 IEEE International Conference on*, 1992, pp. 1300-1305 vol.2.

- [13] R. F. Santos, P. F. Rocha, S. Lanceros-Mendez, C. Santos, and J. G. Rocha, "3 Axis Capacitive Tactile Sensor," in *Industrial Electronics, 2005. ISIE 2005. Proceedings of the IEEE International Symposium on*, 2005, pp. 1539-1544.
- [14] K. Laws, "Physics and the Art of Dance: Understanding Movement," *Physics Today*, vol. 56, pp. 64-64, 2003.
- [15] S. D. Brown, "Laboratory robotics: A guide to planning, programming and applications, W. Jeffrey Hurst and James W. Mortimer, VCH Publishers, Inc., Deerfield Beach, FL, U.S.A., 1987. ISBN 0-89573-322-6. Price: US\$24.95," *Journal of Chemometrics*, vol. 2, pp. 298-298, 1988.
- [16] J. G. Liscouski, *Laboratory and scientific computing : a strategic approach*. New York: Wiley, 1995.
- [17] F. Balena, *Programming Microsoft Visual Basic .NET version 2003*. Redmond, Wash.: Microsoft Press, 2004.